Hydrological Sciences Journal

ISSN: 0262-6667 (Print) 2150-3435 (Online) Journal homepage: https://www.tandfonline.com/loi/thsj20

How do potential evapotranspiration formulas influence hydrological projections?

G. Seiller & F. Anctil

To cite this article: G. Seiller & F. Anctil (2016) How do potential evapotranspiration formulas influence hydrological projections?, Hydrological Sciences Journal, 61:12, 2249-2266, DOI: 10.1080/02626667.2015.1100302

To link to this article: https://doi.org/10.1080/02626667.2015.1100302

HYDROLOGICAL SCIENCES JOURNAL – JOURNAL DES SCIENCES HYDROLOGIQUES, 2016
VOL. 61, NO. 12, 2249–2266
http://dx.doi.org/10.1080/02626667.2015.1100302

How do potential evapotranspiration formulas influence hydrological projections?

G. Seiller and F. Anctil

Département de génie civil et de génie des eaux, Université Laval, Québec, Canada

ABSTRACT

This paper evaluates the sensitivity of hydrological projections to the choice of potential evapotranspiration formulas on two natural sub-catchments, in Canada and Germany. Twenty-four equations, representing a large range of options, are applied for calibration over the whole observation time series and for future conditions. The modelling chain is composed of dynamically downscaled climatic projections and a 20-member (ensemble) hydrological model, along with a snow module. The roots of the sensitivity and its propagation within the hydrological chain are evaluated to show influences on climate change impact conclusions. Results show large differences between the 24 simulated potential evapotranspiration time series. However, these discrepancies only moderately affect the calibration efficiency of hydrological models as a result of adaptation of parameters. Choice of formula influences hydrological projections and climate change conclusions for both catchments in terms of simulated and projected values, and also in the magnitude of changes during important dynamic periods such as spring and autumn high flows and summer low flows. Spread of the hydrological response is lower for the combinational formulas than for temperature-based or radiation-based equations. All the results reveal the importance of testing a large spectrum of potential evapotranspiration formulas in a decision-making context, such as water resources management.

ARTICLE HISTORY
Received 3 July 2014
Accepted 21 September 2015

EDITOR
Z.W. Kundzewicz

ASSOCIATE EDITOR
not assigned

KEYWORDS
potential evapotranspiration; hydrological modelling; climate change; uncertainty; future projection

1 Introduction

Quantifying the impacts of climate change on the hydrological cycle and evaluating related uncertainties remains a major challenge. Proper quantification of these uncertainties is essential for a risk-based approach in a decision-making context, such as water resources management (Kay *et al.* 2009). In a conceptual way, Hulme *et al.* (1999) identified two categories of uncertainties in climate change impact and adaptation studies: "incomplete" knowledge, reflected by model conceptualization, and "unknowable" knowledge, related to human and the climate system behaviours. Indeed, the scientific community considers that any study of climate change impacts on water resources involves four broad levels of uncertainty (Maurer 2007, Boé *et al.* 2009). The first three levels concern the production of climatic scenarios at the catchment scale: gas emission scenarios, global climate model (GCM) outputs, and downscaling techniques used to adapt data to the catchment scale. The fourth level involves the impact of the hydrological modelling tools. Some studies embedded all levels of uncertainty (e.g. Prudhomme *et al.* 2003, Dibike and Coulibaly 2005; Maurer 2007, Vicuna *et al.* 2007, Minville *et al.* 2008, Kay *et al.* 2009, Boyer *et al.* 2010), whereas others focused on some of them (e.g. Georgakakos *et al.* 2004, Jones *et al.* 2006, Gardner 2009, Ludwig *et al.* 2009, Milly and Dunne 2011, Seiller and Anctil 2014). All four levels of uncertainty include their own inner ones. Hydrological modelling uncertainties depend mainly on inputs (measurements and estimations), model structure (conceptualization and complexity) and parameter uncertainty (equifinality, parameter identifiability, transposability). Input uncertainties originate from rainfall, temperature and other meteorological data measurements, as well as evapotranspiration estimations. This latter part of the hydrological modelling sequence has been sparsely studied in the context of climate change impacts, even though the evaporative demand remains a pivotal question when addressing future climate.

1.1 Potential evapotranspiration for hydrological modelling in a climate change context

At the Earth scale, annual precipitation amounts to 750 mm/year, of which two-thirds returns to the atmosphere from the land surface via evapotranspiration, making it a key element of the terrestrial hydrological cycle (Baumgartner *et al.* 1975). Combined understanding of precipitation and evapotranspiration at the catchment scale is, therefore, a prerequisite to hydrological modelling.

1.1.1 Potential evapotranspiration

The potential evapotranspiration (PET) concept was first introduced by Thornthwaite (1948) for climate classification and was next popularized in agriculture and water resources as a prior calculation to the actual evapotranspiration (AET). Penman (1948) was the first to propose a calculation method to estimate evaporation from open water, bare soil and grass, later associated with the PET concept. Even if many different definitions have been proposed depending on the context, in a conceptual way potential evapotranspiration is the maximum

CONTACT G. Seiller gregory.seiller.1@ulaval.ca

possible evapotranspiration rate that can occur from a continuously saturated surface under ambient meteorological conditions (Thornthwaite 1948, Lhomme 1997). Thus, if sufficient water is available to meet the sum of evaporation and transpiration, the evapotranspiration will reach its maximum potential value. Otherwise, the AET will be less than the PET.

More recently, the reference evapotranspiration concept (ET_0) emerged; this is considered as the rate at which readily available soil water is vaporized from a specified vegetation surface (Jensen *et al.* 1990). This concept leads to PET when multiplied by an appropriate crop coefficient (K_c), developed to standardize estimation of crop water use and representing variations in stomatal control by the plants and the aerodynamic resistance. When applied on catchments where land-use data are not available or not taken into account (e.g. lumped modelling), this crop coefficient cannot be estimated (Bos *et al.* 2009) and the PET concept is used.

Nowadays, PET formulas exist in abundance, reflecting the difficulty of condensing this turbulent process into a simple expression. They may be classified into five groups (Xu and Singh 2001): (1) water budget, (2) mass transfer, (3) combinational, (4) radiation-based and (5) temperature-based.

1.1.2 Options for the estimation of evapotranspiration

The many PET formulas, the substantial data needed, and the level of required expertise make it difficult to select the most appropriate formula for a given situation. Consequently, they are often analysed and compared for a specific system, as illustrated by Verstraeten *et al.* (2008). Numerous scientists took a similar path, for example Brutsaert (1982), Singh (1989), Jensen *et al.* (1990), Morton (1994), Singh and Xu (1997a), Xu and Singh (2000, 2001, 2002), Fisher *et al.* (2005), Oudin *et al.* (2005a, 2005b) and Donohue *et al.* (2010) and. In these studies, evapotranspiration is calculated from several assumptions and rationales, from aerodynamic, energy balance, combined aerodynamic–energy balance, to empirical formulas. The combinational Penman formula (or its Penman-Monteith variant) is often used as a benchmark because of its recognized agreement with lysimeter measurements (Jensen *et al.* 1990, Oudin *et al.* 2005a). Moreover, it has been identified as the most satisfying formula by the FAO (Allen *et al.* 1998) and the ASCE (Allen *et al.* 2005), and is used by numerous weather services. However, some authors (for example Singh and Xu 1997b) showed that this more comprehensive formula only leads to better estimates if the input variables are well measured or estimated.

1.1.3 Application in hydrological modelling

Projects looking at evaluating the sensitivity of hydrological models to PET formulas are quite scant in the scientific literature, even if some recent works have filled this gap (Andréassian *et al.* 2004, Oudin *et al.* 2005a, 2005b, Kannan *et al.* 2007, Kay and Davies 2008). For instance, Parmele (1972) stated that one of the principal problems in hydrological model development is the poor knowledge of the sensitivity to PET, which influences discharge as well as the other components of the water cycle. Parmele showed that a constant bias in PET has a cumulative impact and can lead to significant error on hydrological peaks and recession characteristics. However, subsequent studies illustrated that these PET biases may be compensated by hydrological models during the calibration process, adjusting parameters to inputs, as stated for example by Paturel *et al.* (1995). Andréassian *et al.* (2004) confirmed this sensitivity to PET, as the production storage parameters adjust to different scenarios. These results are in a way reassuring, because imperfect PET may still lead to correct discharge simulation. They are also quite confusing and counterintuitive if a better PET does not lead to a better discharge simulation.

These findings were corroborated and extended by Oudin *et al.* (2005a, 2005b). Their first paper, based on the Penman formula (Penman 1948), showed that temporally varying PET and daily averaged PET produce similar discharge time series, as already mentioned by several authors, but based on fewer extensive tests (Edijatno 1991, Burnash 1995, Fowler 2002). In their companion paper, Oudin *et al.* (2005b) tested 27 PET formulas and their simulated discharge influence. They concluded that most PET formulas lead to similar performance, illustrating the low sensitivity of hydrological models to PET selection. However, formulas based on temperature and radiation offered the best results, in contrast to the ones relying on wind speed and relative humidity. The McGuinness (McGuinness and Bordne 1972) and Jensen-Haise (Jensen and Haise 1963) formulas appeared to be the most pertinent ones, better than the Penman formula. These results illustrated interest in simple PET formulas (less physically based) for discharge simulation, as also reported by Kannan *et al.* (2007) and Kay and Davies (2008).

1.1.4 Evapotranspiration in a climate change context

Evaporative demand depends on four major physical variables for which long-term climate change trends show particular influences: air temperature (GIEC 2007), vapour pressure (Durre *et al.* 2009), net radiation (Wild 2009) and wind speed (McVicar *et al.* 2008, 2012). These changes will have a considerable impact on the evaporative demand, as illustrated by Donohue *et al.* (2010). The selection of a pertinent PET formula, which combines these variables in a specific way, may thus be critical. This has been illustrated by McKenney and Rosenberg (1993), who estimated the sensitivity of eight distinct PET formulas at five sites in the North American Great Plains. Results show that very different conclusions on the impacts of climate change can be drawn depending on the formula used, potentially affecting runoff changes. On a larger scale, Sheffield *et al.* (2012) showed the discrepancies in analysis of global drought changes between temperature-based (Thornthwaite) and physically based (Penman) PET formulas in Palmer Drought Severity Index calculation. Kay and Davies (2008) found that the Penman formula and Oudin's temperature-based formula lead to quite different results when applied in a climate change context: scenario A2 for 2071–2100. Kingston *et al.* (2009) investigated six different PET formulas, simulating how they react to an increase in global mean temperature. They reveal PET selection as a major source of uncertainty in projections of future water resources. Bae *et al.* (2011) used three semi-distributed hydrological models and seven PET formulas in their work and concluded that

these tools affect runoff change simulations with larger discrepancies for the 2071–2100 future period. Additionally, Bormann (2011) compared 18 PET formulas with respect to their sensitivity to historical climate change over six German climate stations. Results showed that PET is affected by observed climate change, without the possibility to group these sensitivities in terms of different types of PET. Sperna Weiland *et al.* (2012) also stressed the importance of testing PET formulas over the studied catchments and found better model performance using the simplest formulas in contrast to the combinational ones, thus limiting the number of input variables in a climate change data demanding context. Prudhomme and Williamson (2013) compared 12 PET formulas driven by the HadRM3 regional climate model over Great Britain and also illustrated a large variation of the changes, both in magnitude and sometimes direction, from the different PET options. All these results confirmed the necessity to test different PET options to encompass the challenge of evaporative demand uncertainty.

Moreover, evaporative demand changes can also occur through changes in transpiration controls (Kay *et al.* 2013), where variations in the concentration of CO_2 in the atmosphere can lead to plant physiological changes, such as stomata opening or plant growth (i.e. changes in leaf area, number of stomata). These relationships between meteorology, plant physiology and climate change can be very complex and result in additional uncertainties and effects on diagnosis of impacts, as illustrated for example by Betts *et al.* (2007), Bell *et al.* (2011, 2012) and Kay *et al.* (2013).

1.2 Objectives

The literature identifies the importance of evaporative demand evaluation in a climate change context, as well as the complexity linked with this task, especially in such situations for which climatic variables affecting evapotranspiration may potentially have a cumulative influence. In this context, the selection of an adapted evapotranspiration equation as input for hydrological modelling may be difficult and need special attention. Questions thus arise about our ability to produce a diagnosis of climate change impacts on water resources. More specifically, this paper explores the sensitivity of hydrological projections to the choice of PET formulas among 24, over a catchment in Canada and another one in Germany, based on available meteorological observations and climate model data for the reference (1970–2000) and future (2041–2070) periods, and on the 20-lumped-model ensemble set-up by Seiller *et al.* (2012). This ensemble set-up is based on a deterministic averaging of all individually calibrated hydrological model outputs.

Because the *a priori* choice of an appropriate PET formula, even for a specific location and climate conditions, is not an obvious task, the assessment resorts to diverse available options for evapotranspiration estimation. Even if some studies have concluded that adjustment of model parameters (i.e. during the calibration process) reduces the sensitivity of hydrological modelling to PET, it has not been extensively assessed in the context of hydrological projection, for which one desires a model that performs well for the right reasons (Kirchner 2006).

2 Material and methods

2.1 Studied catchments

Two catchments are studied: au Saumon from the upper Saint-François River in the Province of Québec (Canada) and Schlehdorf from the upper Isar River in the State of Bavaria (Germany). These snow-influenced watersheds have dissimilar hydrological behaviour mainly originating from contrasted precipitation, temperature conditions and topographical characteristics. The Canadian site is subject to a snowmelt maximum in spring and high discharges in autumn, while the German watershed is characterized by alpine snowmelt in spring associated with a strong summer precipitation maximum. Both are studied in partnership with the QBIC^3 project (Quebecer and Bavarian modelling Intercomparison). They are relatively anthropogenically undisturbed sections of their respective rivers.

The au Saumon catchment (Fig. 1) drains 738 km^2 with a snowmelt maximum in spring and a high discharge in autumn. Annual precipitation reaches 1284 mm/year (calculated from 1975 to 2003), including 355 mm/year of snow, resulting in an annual discharge of 771 mm/year. Altitudes range from 277 to 1092 m a.s.l., with a mean temperature of 4.5°C, while land use mainly consists of coniferous and deciduous forests and croplands on limestone, sandstone and shale.

The Schlehdorf catchment (Fig. 2) drains 708 km^2 of alpine land, with snowmelt in spring and strong summer precipitation. Annual precipitation totals 1420 mm/year, among which 347 mm/year are snow (computed from 1970 to 2000). The mean annual temperature is 5.2°C and the annual discharge reaches 983 mm/year. Its altitude ranges from 603 to 2562 m a.s.l., while land use is mainly coniferous and deciduous forests and rocks, on limestone and dolomite.

This study did not take directly into account the effect of land-use evolution on both catchments between the historical and future periods, mainly because conceptual lumped models are not dedicated to this type of analysis and because no related information is available on the catchments.

2.2 Meteorological and climatic data

Observation data (OBS), also called baseline data, consist of daily lumped air temperature (mean, min and max, in °C), precipitation (in mm), incoming solar radiation (in W/m^2), relative humidity (in %) and 2-m wind speed (in m/s). OBS (1975 to 2003 for au Saumon and 1970 to 2000 for Schlehdorf) are used for direct comparison with the climatic data (see Fig. 3), for PET comparison and for calibration. Precipitation and temperature data are averaged from 13 meteorological stations for au Saumon and 6 stations for Schlehdorf. Radiation, humidity and wind speed data originate from Sherbrooke and Bad Toelz, for au Saumon and Schlehdorf, respectively. Data were provided and validated by

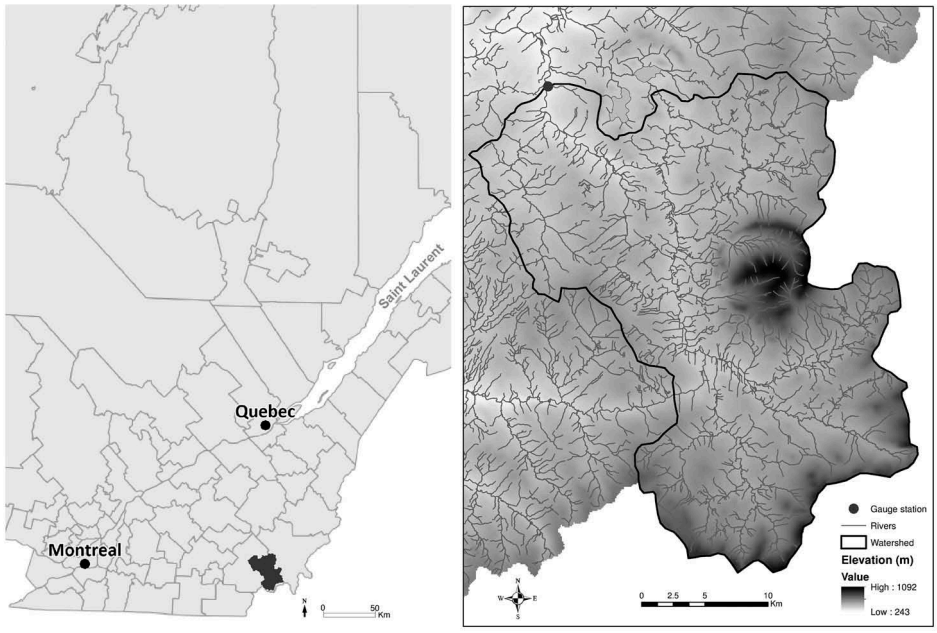

Figure 1. Location of the au Saumon catchment (738 km^2; Canada).

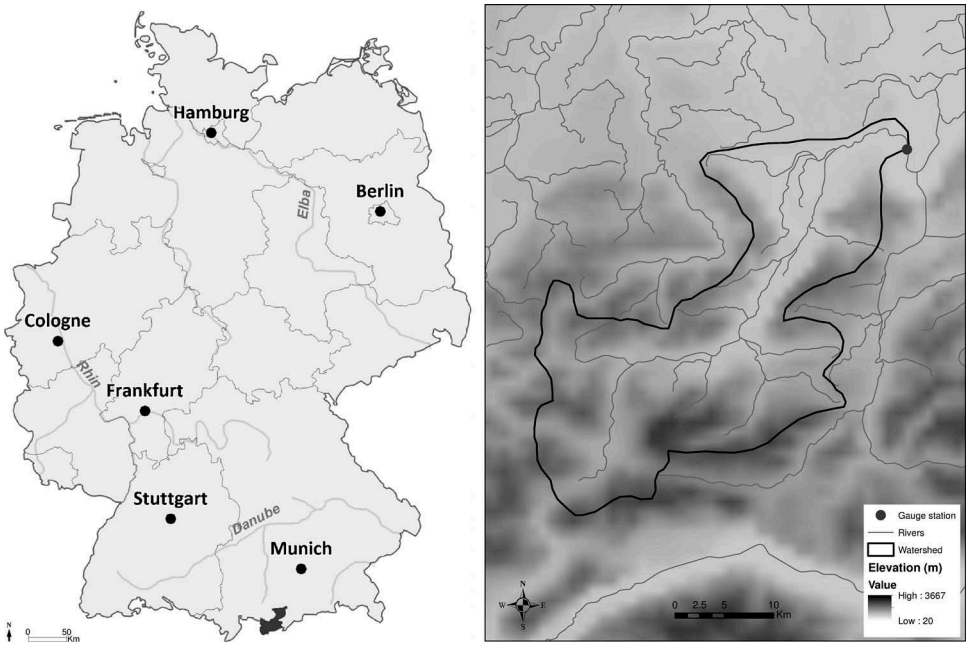

Figure 2. Location of the Schlehdorf catchment (708 km^2; Germany).

the Centre d'Expertise Hydrique du Québec (Canada) and by the Ludwig-Maximilians-Universität (Germany).

Climatic data originated from the Canadian Global Climate Model (CGCM version 3) driven by the SRES A2 scenario (Nakicenovic *et al.* 2000), dynamically downscaled by the Canadian Regional Climate Model (CRCM version 4.2.3) over a 45-km grid (De Elía and Côté 2010) with 29 vertical layers and running at a 15-minute time step. These climatic data are available for the reference (REF, 1971–2000) and future (FUT, 2041–2070) periods. Five climatic members are available from the CGCM but, since only the fourth one has been downscaled over Germany, the latter is selected here for both catchments.

Statistical downscaling follows the SCALMET (SCAling METeorological variables) procedure: an algorithm (Marke 2008) allowing discretization to 1 km^2 that conserves mass and energy within a CRCM grid cell when downscaling to hydrological scale (Muerth *et al.* 2013). Bias correction aims to improve air temperature and precipitation time series, computing monthly correction factors for all the available members. This correction is based on differences between observed (i.e. meteorological) and reference climatic mean monthly air

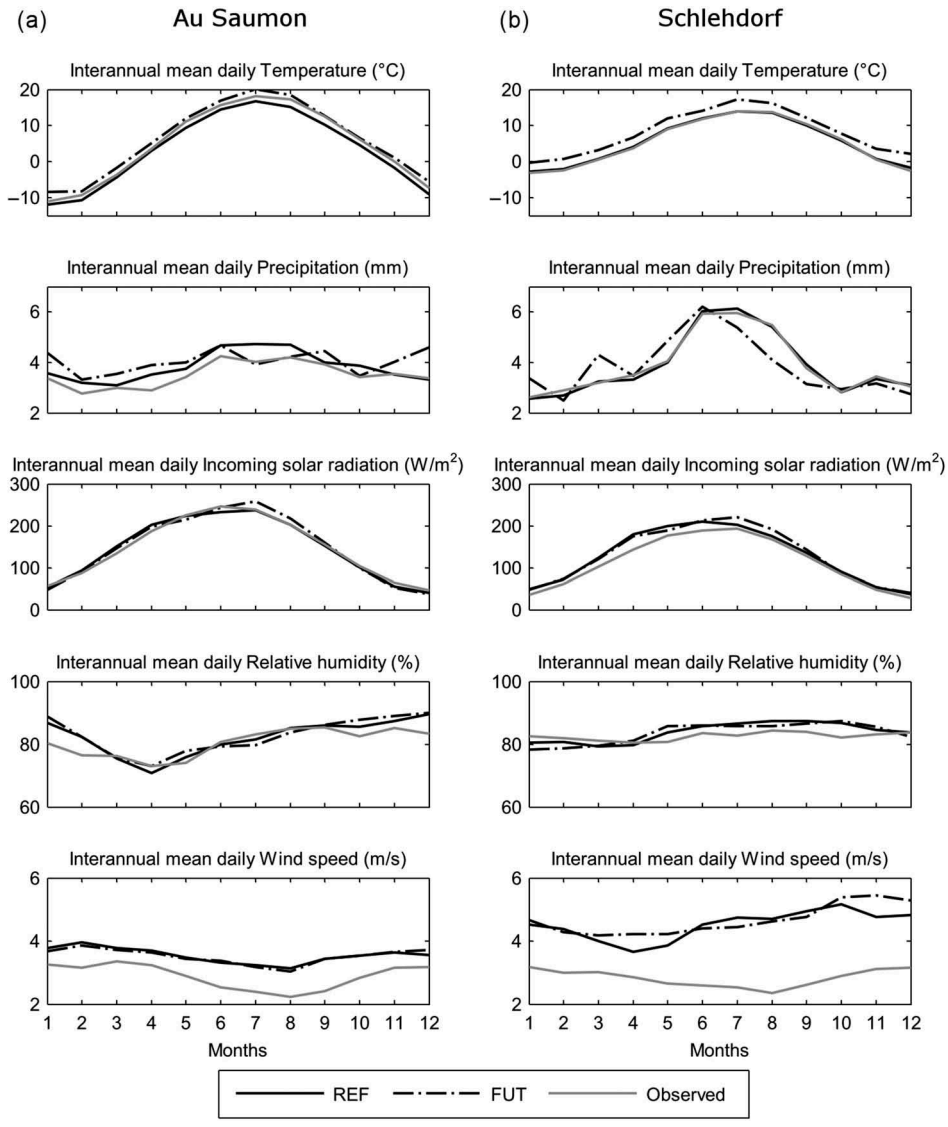

Figure 3. Mean daily meteorological and climatic input data for (a) au Saumon and (b) Schlehdorf catchments. Grey lines are observed data, black lines REF data (1971–2000) and dashed lines FUT data (2041–2070).

temperature (30-year average), and for precipitation by using the LOCI method (LOCal Intensity scaling) as described in Schmidli *et al.* (2006). Bias correction is limited to precipitation and temperature where data are the most reliable in this lumped context. Several shortcomings are, however, associated with the bias correction process as for example stated by Ehret *et al.* (2012), Muerth *et al.* (2013) or Fischer and Knutti (2013). One of them is based on some consistency loss during bias correction, as it is statistical, especially when only some variables are corrected. Also, the assumption that the correction parameters computed in the past period will remain the same for future periods is an arguable hypothesis. Ongoing work by collaborators for this project specifically addresses the bias correction issue (e.g. Chen *et al.* 2013, Muerth *et al.* 2013).

2.3 Hydro-climatic modelling chain

Production of OBS, REF and FUT flow simulations involves several modelling processes and tools. Air temperature, incoming solar radiation, relative humidity and 2-m wind speed are possible inputs to PET formulas. Air temperature and precipitation are inputs to the CemaNeige snow accounting module (Valéry *et al.* 2014), which provides melt as output. Liquid precipitation, melt and PET are inputs to the hydrological model simulating discharge.

2.3.1 Potential evapotranspiration formulas

The 24 PET formulas (Table 1) are of three types: combinational, temperature-based and radiation-based. Temperature-based and radiation-based formulas are empirical, whereas combinational ones mix energetic and mass-transfer concepts. The adopted classification depends more heavily on the philosophy of development than on the inputs. For example, the E_{04} (Priestley-Taylor) formula belongs to the combinational class even if the wind speed input is not used, because it is a simplification of Penman's equation. On the other hand, since the E_{20} formula (Doorenbos-Pruitt) is an adaptation of the radiation-based formula E_{22} (Makkink), it belongs to the radiation-based class even if it asks for the wind speed.

Table 1. List of the 24 PET formulas by category: combinational, temperature-based and radiation-based.

PET class	Short name	Formula name	Required data
Combinational	E_{01}	Penman	RH, T, U, Rs
	E_{02}	Penman-Monteith	RH, T, U, Rs
	E_{03}	FAO56 P-M (ASCE)*	RH, T, U, Rs
	E_{04}	Priestley-Taylor	T, Rs
	E_{05}	Kimberly-Penman*	RH, T, U, Rs
	E_{06}	Thom-Oliver	RH, T, U, Rs
Temperature-based	E_{07}	Thornthwaite	T
	E_{08}	Blaney-Criddle	T, Rs
	E_{09}	Hamon	T, Rs
	E_{10}	Romanenko	RH, T
	E_{11}	Linacre	RH, T
	E_{12}	MOHYSE	T
	E_{13}	Hydro-Québec (HSAMI)	T
	E_{14}	Kharrufa	T
Radiation-based	E_{15}	Wendling (WASIM)	T, Rs
	E_{16}	Turc	RH, T, Rs
	E_{17}	Jensen-Haise	T
	E_{18}	McGuinness-Bordne	T
	E_{19}	Hargreaves	T
	E_{20}	Doorenbos-Pruitt	RH, T, U, Rs
	E_{21}	Abtew	RH, T, Rs
	E_{22}	Makkink	T
	E_{23}	Oudin	T
	E_{24}	Baier-Robertson	T

RH: relative humidity; T: temperature; U: wind speed; Rs: incoming solar radiation
*Based on reference ET concept (ET_0)

Details of the 24 PET formulas are provided in the Appendix. The intermediary physical, meteorological and atmospheric parameters have mainly been calculated based on the EWRI-ASCE report (Allen *et al.* 2005). When available, empirical coefficients have been selected according to the project catchments in order to compute "the most accurate and spatially stable PET method", as mentioned by Sperna Weiland *et al.* (2012).

2.3.2 Ensemble of 20 lumped hydrological models

In our specific context, hydrological models are the inference tools for PET assessment and must be well suited for catchment simulation, without favouritism towards any PET formula. A combination of modelling concepts is adopted here: 20 lumped conceptual hydrological models (see Table 2)—some have been transformed to a lumped mode—pooled in a deterministic way to form an ensemble (the output of the multimodel is the average of the output of each individual model). Selected individual models are structured around four to ten free parameters and two to seven storage units, taking into account soil moisture (linear and nonlinear computation, with one or several layers) and exploiting routing components (linear and nonlinear, with unit hydrographs or time delays). Most of them were developed by Perrin *et al.* (2001), Mathevet (2005), Velázquez *et al.* (2010, 2011) or Seiller *et al.* (2015). Given the amount of simulations needed, these parsimonious models were preferred over distributed and physically based ones.

In previous work on the same two catchments, Seiller *et al.* (2012) showed that this 20-member ensemble offers good performance and robustness for contrasting climate conditions. It is advocated that the proposed multimodel is more neutral to the PET than any individual model, increasing the chance that any difference in discharge simulation be attributed to the PET and not the hydrological model.

2.3.3 Snow module

Snow accumulation and melt are simulated by the CemaNeige snow module (Valéry *et al.* 2014). This two-parameter module is based on a degree-day approach over five altitudinal layers of equal area, while temperature and precipitation are extrapolated using altitudinal gradients, and the distinction between liquid and solid precipitation relies on altitudinal temperature. Two internal state variables of the snowpack for each zone are simulated: the thermal state and the melting potential.

2.4 Model calibration and validation performance

The hydrological models are calibrated individually along with the CemaNeige snow module, exploiting all available observations. Each model is calibrated with the 24 PET formulas resulting in 480 parameter sets. The calibration process (CAL) is based on the automatic optimization method known as the shuffled complex evolution (SCE) (Duan *et al.* 1992,

Table 2. Main characteristics of the 20 hydrological models.

Model name	Model acronym	Number of optimized parameters	Number of storages	Derived from
M01	BUCK	6	3	BUCKET (Thornthwaite and Mather 1955)
M02	CEQU	9	2	CEQUEAU (Girard *et al.* 1972)
M03	CREC	6	3	CREC (Cormary and Guilbot 1973)
M04	GARD	6	3	GARDENIA (Thiery 1982)
M05	GR4J	4	3	GR4J (Perrin *et al.* 2003)
M06	HBV0	9	3	HBV (Bergström and Forsman 1973)
M07	HYMO	6	5	HYMOD (Wagener *et al.* 2001)
M08	IHAC	7	3	IHACRES (Jakeman *et al.* 1990)
M09	MART	7	4	MARTINE (Mazenc *et al.* 1984)
M10	MOHY	7	3	MOHYSE (Fortin and Turcotte 2006)
M11	MORD	6	4	MORDOR (Garçon 1999)
M12	NAM0	10	7	NAM (Nielsen and Hansen 1973)
M13	PDM0	8	4	PDM (Moore and Clarke 1981)
M14	SACR	9	5	SACRAMENTO (Burnash *et al.* 1973)
M15	SIMH	8	4	SIMHYD (Chiew *et al.* 2002)
M16	SMAR	8	4	SMAR (O'Connell *et al.* 1970)
M17	TANK	7	4	TANK (Sugawara 1979)
M18	TOPM	7	4	TOPMODEL (Beven and Kirkby 1979)
M19	WAGE	8	3	WAGENINGEN (Warmerdam *et al.* 1997)
M20	XINA	8	5	XINANJIANG (Zhao *et al.* 1980)

1994). The objective function is the root mean square error applied to root-squared transformed discharge ($RMSE_{sqrt}$).

$$RMSE_{sqrt} = \sqrt{\frac{\sum_{i=1}^{N}\left(\sqrt{Q_{sim,i}} - \sqrt{Q_{obs,i}}\right)^2}{N}} \quad (1)$$

where $Q_{obs,i}$ and $Q_{sim,i}$ are respectively the observed and simulated streamflows at time i and N is the number of observations. Evaluation on root-square discharge allows a multi-purpose analysis focusing on the adequacy of the entire simulated hydrograph between observed and simulated discharges, by more evenly weighting high and low flows (Chiew and McMahon 1994, Oudin *et al.* 2006).

In order to evaluate performance, the adequacy between observed and simulated discharges in CAL, the Nash-Sutcliffe efficiency is used, calculated on root-squared transformed streamflows for the same reason as explained earlier:

$$NSE_{sqrt} = 1 - \frac{\sum_{i=1}^{N}\left(\sqrt{Q_{sim,i}} - \sqrt{Q_{obs,i}}\right)^2}{\sum_{i=1}^{N}\left(\sqrt{Q_{obs,i}} - \overline{\sqrt{Q_{obs}}}\right)^2} \quad (2)$$

in which $\overline{\sqrt{Q_{obs}}}$ is the mean of square root transformed flows. Values range from negative infinity to 1, the value of 1 corresponding to a perfect model simulation.

It must be kept in mind that, when using climatic data as inputs to PET formulas and hydrological models (i.e. reference simulations and future projections), the latter were already set up with observed meteorological data and are thus not submitted again to calibration. Changes between reference simulations and future projections are therefore related to climate trends and the way PET formulas process the data.

2.5 Quantiles analysis

Quantiles are recognized for their robustness and simplicity (Wilcox 1997, Hannachi 2006, Wilks 2011). They are used here for comparison between REF and FUT on discharges. Quantile–quantile plots (q-q plots) are exploited to illustrate differences in distribution between a pair of series. A q-q plot is a scatterplot where each pair of coordinates defining the position of a point consists of a data value for the p quantile for the first time series (for example REF) and the equivalent value for the second one (for example FUT). If the samples do come from the same distribution, the plot will be linear (i.e. in agreement with a 45-degree reference line). Advantages of q-q plots are that the sample sizes do not need to be equal and that the presence of outliers can easily be detected, as well as any shifts in location, scale, or shape of the distributions.

2.6 Hydrological indicators

Hydrological indicators are used to evaluate changes in water resources over a period. In a climate change context, these simple tools illustrate the evolution of water resources over the catchment. The overall mean flow (OMF) consists of a simple daily mean discharge over selected periods:

$$OMF = \frac{1}{N}\sum_{i=1}^{N} Q_{sim,i} \quad (3)$$

where $Q_{sim,i}$ is the simulated streamflow at time i and N is the number of observations. This indicator is also used for summer periods (i.e. June, July and August, named summer OMF) where PET is maximal for both catchments.

3 Results and discussion

3.1 Input data and future changes

Figure 3 illustrates the averaged mean daily meteorological and climatic input data for the two catchments: OBS, REF and FUT periods. Looking at the temperature, we can highlight that REF for au Saumon slightly underestimates values for all months, whereas they are in much better agreement for Schlehdorf. FUT is warmer than REF by 2–3°C for au Saumon and by 3–4°C for Schlehdorf. For precipitation, OBS and REF coincide for Schlehdorf, but REF overestimates summer precipitation for au Saumon. Changes between REF and FUT are noticeable for both catchments. Schlehdorf receives less water from July to September but more in March and May, while au Saumon has higher precipitation from November to May but slightly less in summer. OBS, REF and FUT incoming solar radiation are quite similar for au Saumon, except for some slightly higher values for FUT in June to August. The agreement is not as convincing for Schlehdorf. OBS incoming solar radiation is lower than REF for the entire year, with the largest gap, 36 W/m^2, occurring in April. FUT values are higher from June to September but lower in April and May. OBS and REF relative humidity differ, especially in winter for au Saumon and in summer for Schlehdorf. FUT values are grossly similar to REF ones. Wind speed is overestimated by the climate models. These discrepancies are probably linked to the downscaling process and to the local effect of topography, not represented accurately in climate models. Differences between OBS and REF peak at 0.8 m/s for au Saumon and at 2.4 m/s for Schlehdorf. FUT and REF are quite similar, especially for au Saumon.

3.2 PET time series variability

Simulated PET time series show major dissimilarities between formulas for all periods, as illustrated in Figure 4—note that the OBS-forced denomination is used for the PET series simulated with meteorological input data and REF and FUT with climatic data. As an example, for 1 July on OBS-forced, PET values range from 1.90 to 8.78 mm for au Saumon and from 1.38 to 6.80 mm for Schlehdorf. Disparities express how much the choice of the formula can affect the simulated PET quantities. Annual quantities are also spread over a considerable range: from 376 (E_{02}) to 1456 mm/year (E_{12}) for au Saumon and from 296 (E_{02}) to 1303 mm/year (E_{12}) for Schlehdorf. The three PET classes are identified on Figure 4 using different colours. Combinational formulas lead to quite similar PET quantities and shapes (annual distributions) in both catchments, probably because of structures all emanating from Penman's concept. In contrast, temperature-based formulas provide highly contrasting PET quantities and shapes, from the highest (E_{12}, MOHYSE) to the lowest (E_{10}, Romanenko) in both catchments. Finally, radiation-based

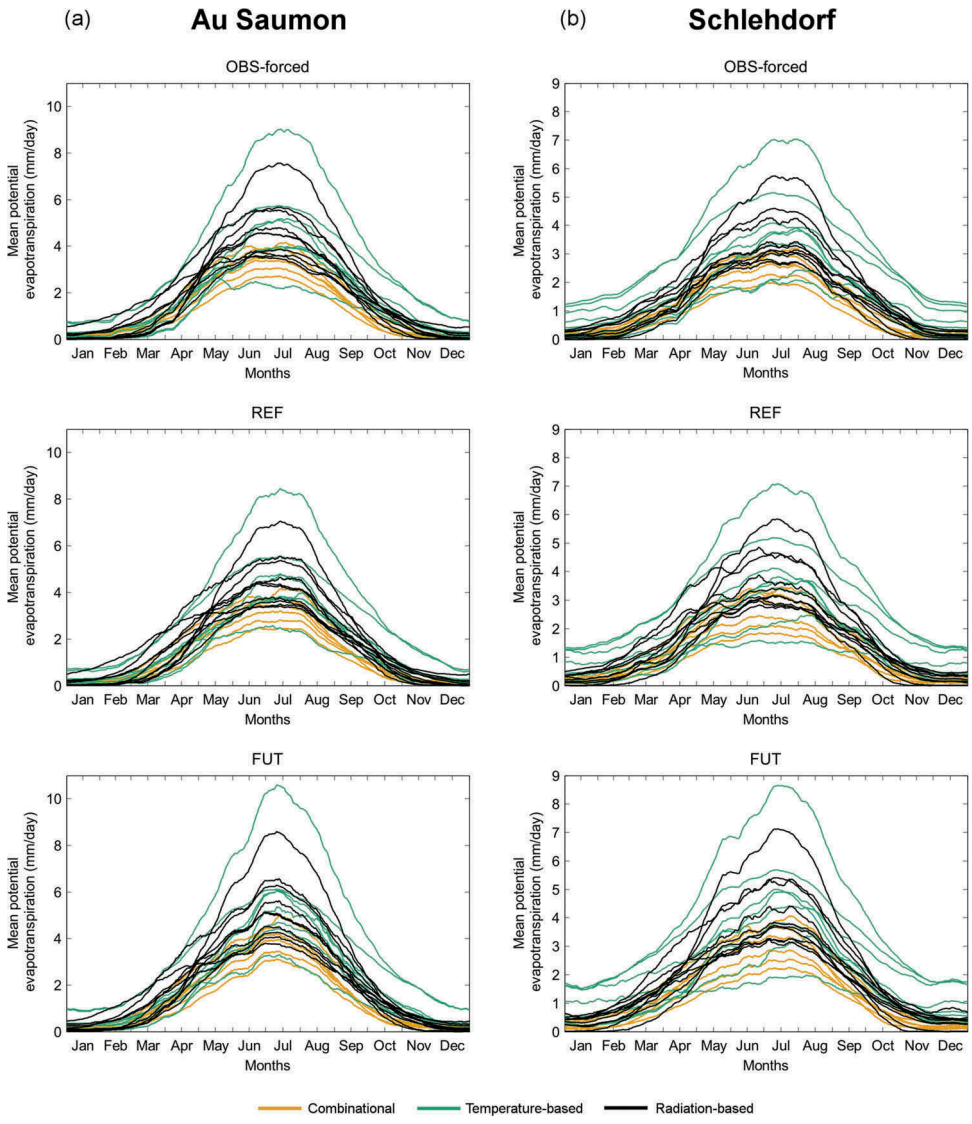

Figure 4. Simulated mean daily potential evapotranspiration series for (a) au Saumon and (b) Schlehdorf catchments, for observed (OBS-forced), reference (REF) and future (FUT) conditions.

formulas (black) are not as widely spread as the temperature-based ones. E_{17} (Jensen-Haise) is the highest radiation-based PET on both catchments. As expected, FUT PET quantities are higher.

Figure 5 groups q-q plots comparing REF and FUT PET time series for au Saumon. In most instances, the absolute increase from REF to FUT is largest for the highest quantiles and quite small for the lowest ones, illustrating a relatively

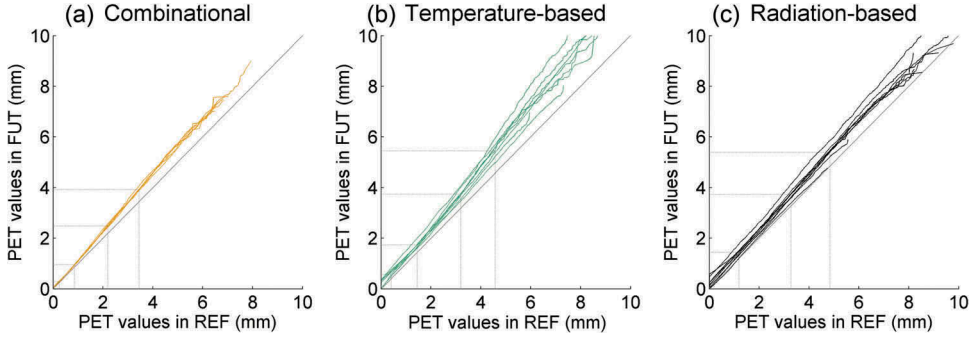

Figure 5. Quantile-quantile plots of the simulated series for 24 PET formulas, by type: (a) combinational, (b) temperature-based, (c) radiation-based, comparing REF with FUT for au Saumon. Dotted lines identify the 25%, 50%, 75% and 90% quantiles.

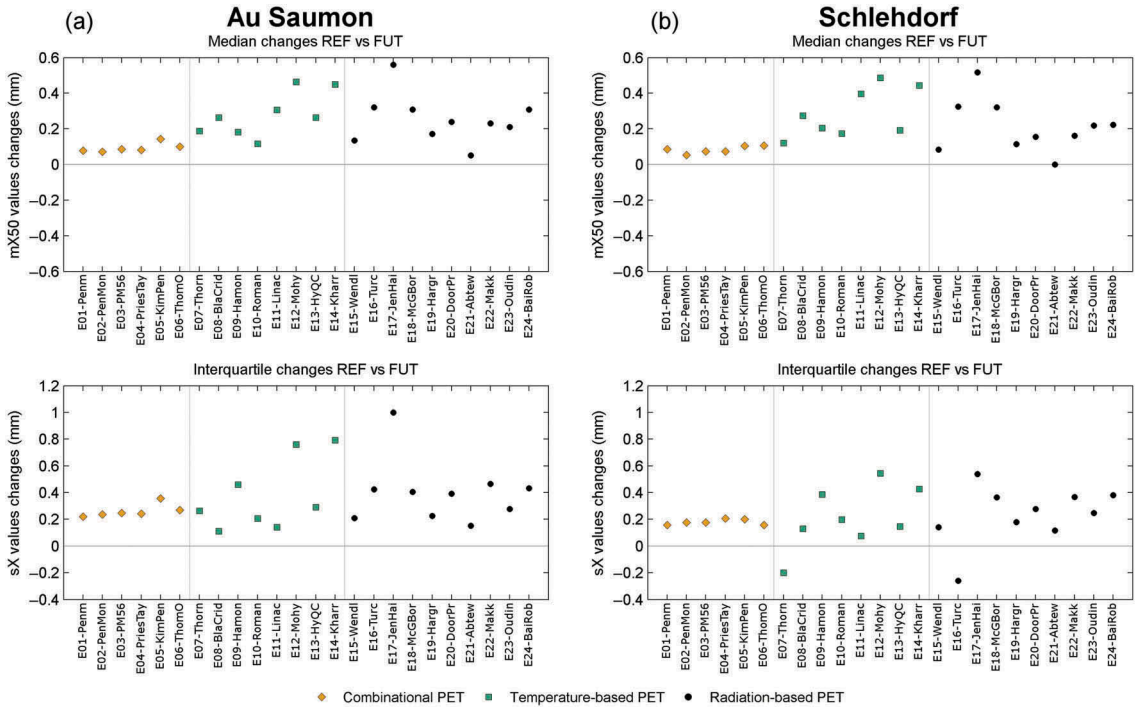

Figure 6. Changes (FUT minus REF) in median and interquartile range for projected PET series for (a) au Saumon and (b) Schlehdorf catchments.

constant percentage of rises generally between +15% (E_{06}) and +25% (E_{13}). Some formulas lead to a more uniform increase, namely E_{07}, E_{08} and E_{24}. Radiation-based E_{21} (Abtew) is the only one faintly responding to climate change (lower line). The Schlehdorf time series (not illustrated) lead to identical comments.

Figure 6 illustrates the median (m×50, 50% quantile) and interquartile range (sX or IQR, difference between 75% and 25% quantiles) evolution for PET from REF to FUT. A similar change in location (increasing in FUT) is noticeable on both catchments, but PET formulas do not have the same sensitivity to climate change. For instance, sensitivity is in general larger for temperature-based and radiation-based formulas. For au Saumon, sX changes also show an increase in FUT, confirming a change in scale, while for Schlehdorf E_{07} and E_{16} show a decrease in sX.

3.3 Simulated discharge series performance

PET sensitivity under observed and future climate conditions is mainly investigated on the simulated discharge, because hydrological modelling is the purpose of the project and also because previous papers (see for example Andréassian *et al.* 2004) have shown that the best representation of PET does not necessarily lead to the best discharge simulation (i.e. adequacy between simulated and observed discharge).

A way to assess the sensitivity and performance of the PET formulas is to compare streamflow calibration efficiency over the entire historical time series (hereinafter referred to as CAL). This calibration process provides the parameter sets for the reference (REF) and future (FUT) simulations and must, in this context, be closely considered. Performance results for both catchments are drawn in Figure 7. Black points illustrate the calibration efficiency of the 20-member hydrological ensemble while boxplots depict the performance range of individual hydrological models, for each PET formula. This way, the general interest of a multimodel approach in terms of performance is again illustrated (black points always in the upper 75% of the boxplots, except for E_{12} on Schlehdorf catchment) and variability of each PET-hydrological model pair is illustrated, allowing the identification of the PET formulas that induce more discharge variability.

For the au Saumon catchment, the hydrological ensemble performance ranges from 0.722 to 0.827. The lowest value originates from temperature-based E_{10} (Romanenko), while the best value is achieved by radiation-based E_{24} (Baier and Robertson) closely followed by temperature-based E_{14} (Kharrufa) and E_{07} (Thornthwaite). Radiation-based equations E_{23} (Oudin) and E_{18} (McGuinness-Bordne) also offer great efficiency for simulated discharges. For their part, individual model performance ranges from 0.020 to 0.834. For Schlehdorf, the multimodel performance ranges from 0.774 to 0.852. The best value is achieved by radiation-based E_{16} (Turc), while the lowest values are obtained for temperature-based E_{08} (Blaney-Criddle) and E_{12} (MOHYSE). Overall, performance values are close for the different PET types, but with higher contrasts for temperature-based formulas, especially for the Schlehdorf watershed. Performance values for the German catchment are higher than for the Canadian one.

These results show that some PET formulas offer superior hydrological performance and smaller individual model variability, resulting in a stable anticipated use for hydrological simulation and projection. Other formulas lead to much greater variability and quite low performance. On the other hand, the 20-member multimodel produces efficient results that are generally more balanced than any individual

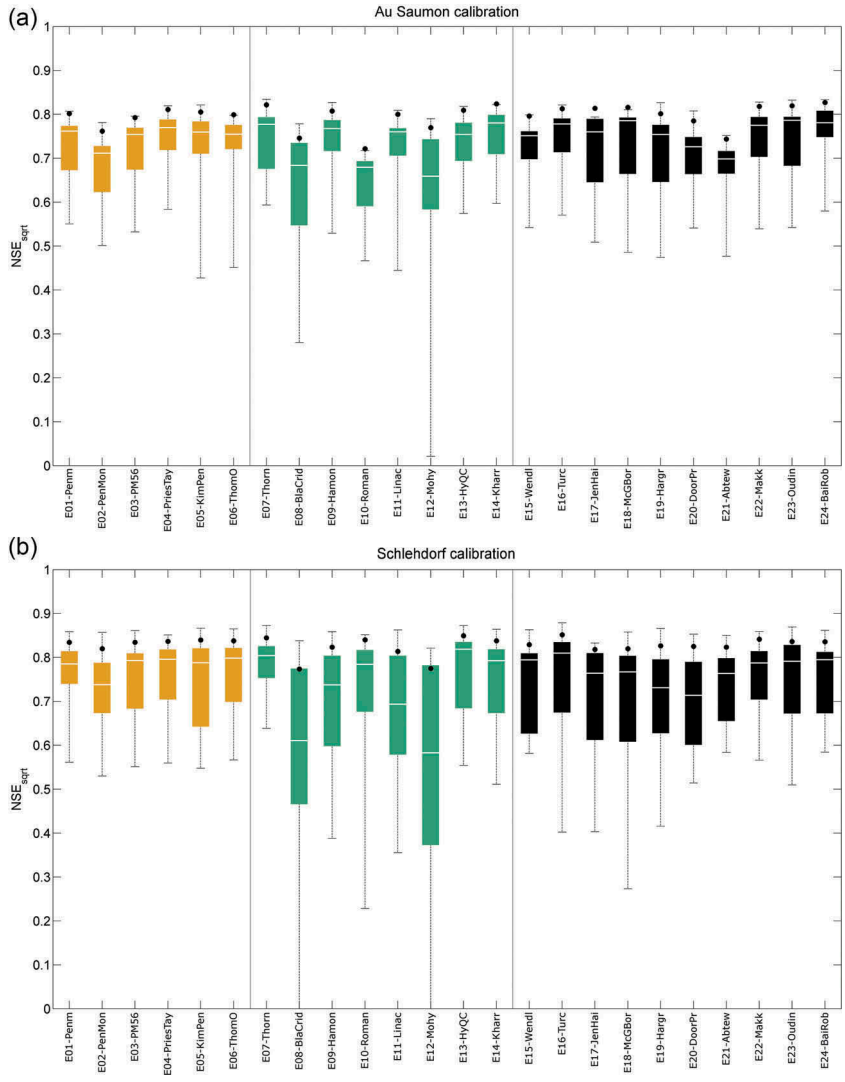

Figure 7. Calibration efficiency (NSE_{sqrt}) on the entire observed datasets for each PET formula and for (a) au Saumon and (b) Schlehdorf. Black points correspond to the 20-member hydrological ensemble and boxplots show the performance range for individual hydrological models.

hydrological model, even if some models sporadically outperform the ensemble (but not always the same model for each PET formula). No clear link can be directly established between PET complexity (i.e. input data and computation steps) and performance but, as already mentioned by several authors, simple formulas often lead to higher calibration efficiency. This statement must, however, be moderated by the fact that more complex formulas also need accurate measurements or estimations of input variables, which remains difficult to assess.

3.4 Analysis on simulated discharge series and quantiles

Figure 8 illustrates the daily averaged discharge observations and simulated time series depicting the variability of the simulation for the different PET formulas and their respective classes.

For au Saumon (Fig. 8(a)), observations are higher than the simulations from November to February, lower from mid-July to the end of September, and similar from March to May. Time series appear ranked by PET classes only from October to February, while radiation-based PET produced the best fit from June to October. The lowest discharge from March to May originates from radiation-based E_{21} (Abtew), a formula that was found to lead to a large volume error. The highest discharge from June to September comes from temperature-based E_{10} (Romanenko). Only temperature-based E_{07} (Thornthwaite) and E_{14} (Kharrufa) reach the observed discharge in April. None of the tested PET formulas can replicate the flow shape from September to December, suggesting that spatial averaging of precipitation data for this time period is not optimal in this lumped modelling context.

For Schlehdorf (Fig. 8(b)), discharge is generally underestimated from mid-June to mid-August and in December, and overestimated from September to the end of October. Larger variability occurs in May and June. Again, analysis by PET class is not obvious because no clear picture emerges. Time series appear ranked by class from September to March, but with small differentiations. Two temperature-based formulas provide small discharge from May to August, E_{08} (Blaney-Criddle) and E_{12} (MOHYSE)—they were responsible for the highest PET (top lines in Figure 4).

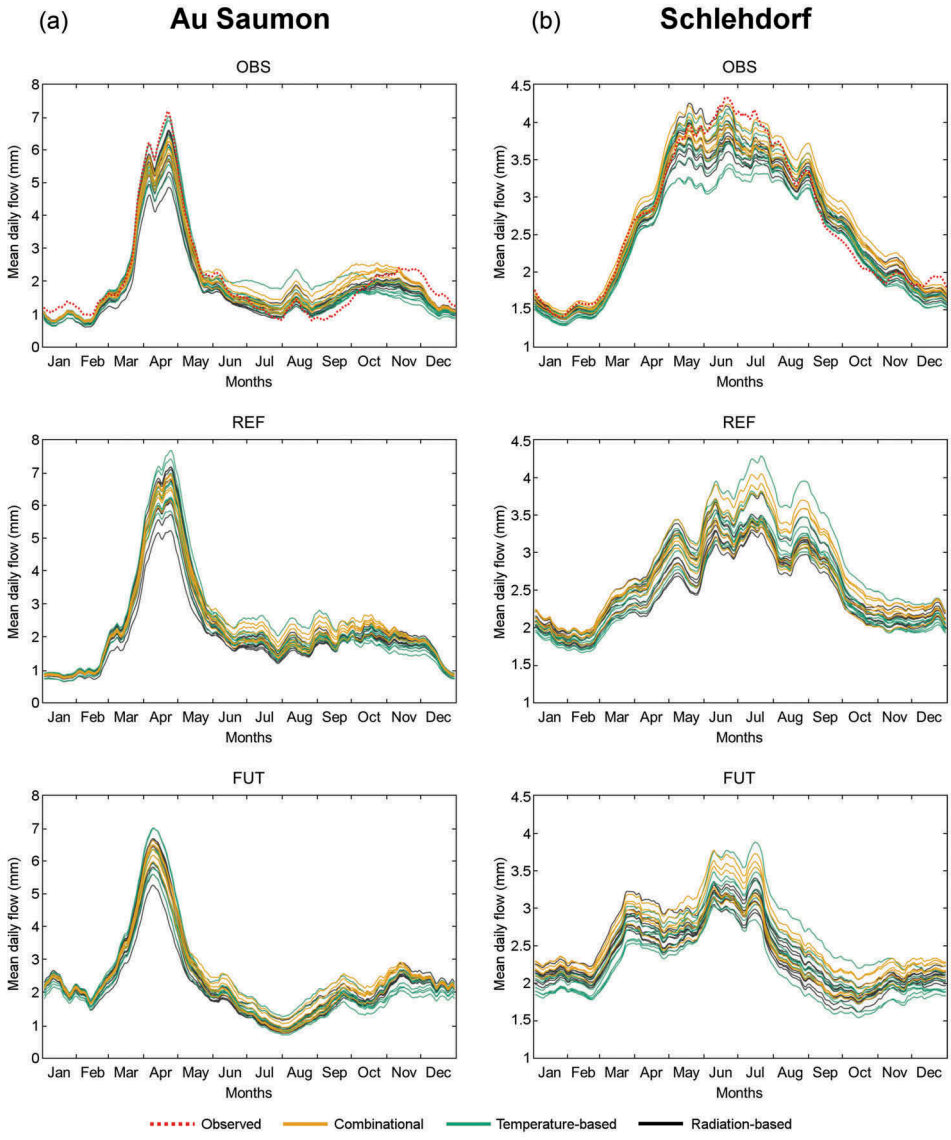

Figure 8. Mean daily simulated flows for (a) au Saumon and (b) Schlehdorf for observed, reference (REF) and future (FUT) conditions, based on the 20-member hydrological model. Red dotted line corresponds to the observed discharge and coloured lines illustrate the sensitivity and families of the 24 PET formulas.

Interestingly, variability is noticeable even for periods with smaller PET, it even reaches a maximum in April. Such behaviour reveals that PET not only affects the water balance at its peak (summer), but influences the parameter identification process to the point of having a year-round impact. Variability in discharge seems directly associated with the adaptation of the model parameters to the PET inputs, more than the real effect of the PET time series (quantity and shape) on water cycle modelling.

Similar envelopes for REF and FUT periods are drawn in Figures 8(a) and (b). PET sensitivity remains in the same range for the two simulated periods.

For au Saumon (Fig. 8(a)), REF has a double peak, capping on day 114 (5.24–7.71 mm), and a summer low flow on day 208 (1.20–2.05 mm). FUT peaks on day 98 with discharges ranging from 5.27 to 7.03 mm and a summer low (day 214) from 0.69 to 1.26 mm. Low flow periods, in winter and summer, show opposite behaviour when projecting from REF to FUT. Winter low flows increase following a higher number of days favourable to liquid precipitation and shorter snowpack duration. Summer low flows decrease because of lower summer precipitation and higher temperature resulting in higher evapotranspiration and an anticipated spring flood.

The Schlehdorf sensitivity envelope (Fig. 8(b)) is less contrasting over the entire year; however, the range of discharge is lower. REF shows an averaged daily hydrograph with no distinguishable single peak. The highest discharge occurs on day 202 (3.25–4.28 mm) and the lowest, day 42 (1.66–1.94 mm). A second low flow period follows in autumn (day 316, from 1.92 to 2.36 mm). FUT differs mainly in anticipated spring flood (day 127 on REF versus day 85 on FUT) and lower flows in summer and early autumn, with a larger sensitivity associated with the PET formulas (low flow, day 288, with values from 1.53 to 2.19 mm). Discharges in winter are slightly higher. Thus, contrasting shifts in annual low flow discharges also occur for Schlehdorf but to a lesser extent than for au Saumon:

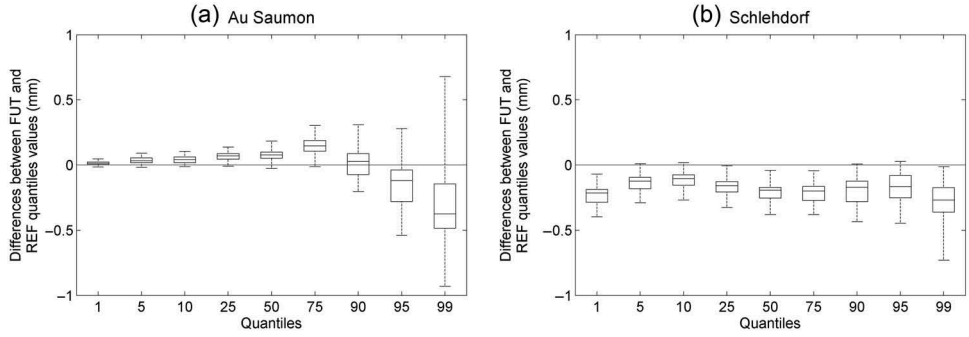

Figure 9. Differences between FUT and REF discharge for 1% to 99% quantiles, for (a) au Saumon, (b) Schlehdorf. Boxplots illustrate the 24 PET formulas.

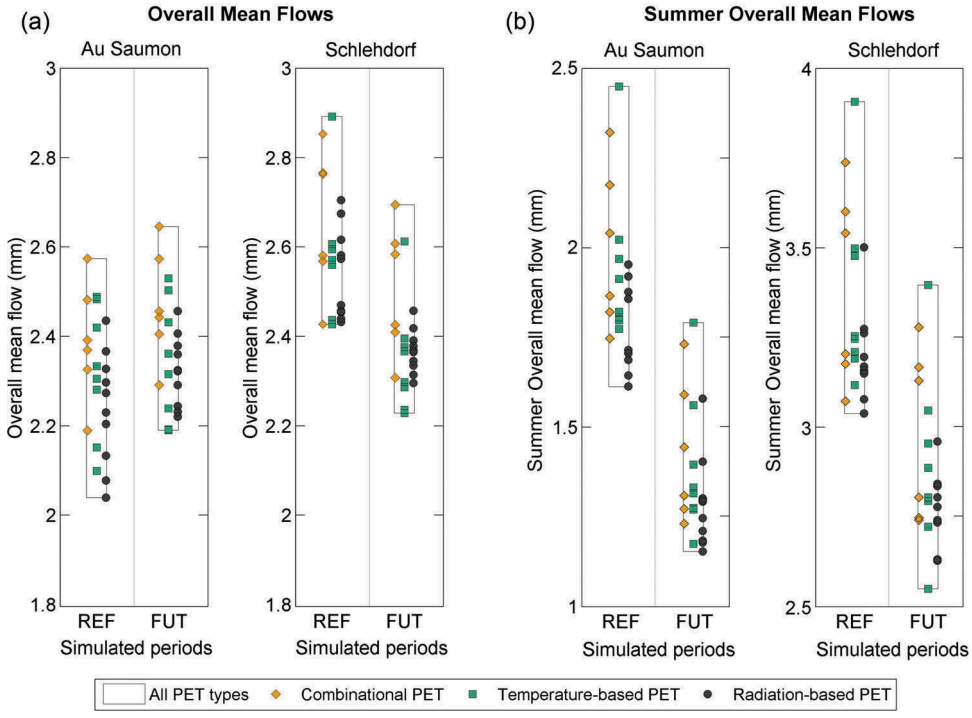

Figure 10. (a) Overall mean flows (OMF) and (b) summer OMF (for June–July–August) for REF and FUT for the 24 PET formulas for both catchments.

lower summer flows and higher winter flows, for similar climatic reasons as for au Saumon.

Figure 9 confirms the dissimilar behaviour of the two catchments. For instance, the sensitivity to PET formula increases with higher quantiles, where occurrence frequency is lower, but mainly for au Saumon. Conclusions in terms of climate change impact are different for both catchments (i.e. higher FUT flows for au Saumon except for some PET formulas and quantiles; lower FUT flows for all PET and smaller sensitivity for Schlehdorf). It must also be mentioned that for au Saumon, especially for the 90, 95 and 99% quantiles, the direction of the change can be positive or negative depending on the PET formula. The apparently unchanged low flow quantiles between REF and FUT in Figure 9, especially for au Saumon, actually hide a reversal of these values. Indeed, as already observed on Figure 8, flows decrease in summer and increase in winter, resulting in a swap of the lower quantiles from REF to FUT period.

3.5 Analysis on hydrological indicators

Hydrological indicators depict the overall impact of climate change on the water cycle and provide an assessment of the sensitivity of the selected 24 potential evapotranspiration formulas. For instance, Figure 10 presents the overall mean flow (OMF) and summer OMF calculated for REF and FUT for both catchments.

Results for OMF (left part) reveal that for au Saumon, the total discharge spread (i.e. height of the bar) is somehow lower for FUT than for REF (0.53 mm for REF and 0.45 mm for FUT), while FUT led to higher overall mean flows (OMF). Combinational PET formulas have a 0.38 mm spread for REF and 0.35 mm for FUT. For temperature-based equations, the results are close in terms of spread (0.39 mm for REF and 0.34 mm for FUT) but their OMF are lower for both periods. Results are, however, slightly different for radiation-based formulas, for which spread is 0.39 mm for REF, but only 0.24 mm for FUT. The highest OMF (REF and FUT) corresponds to

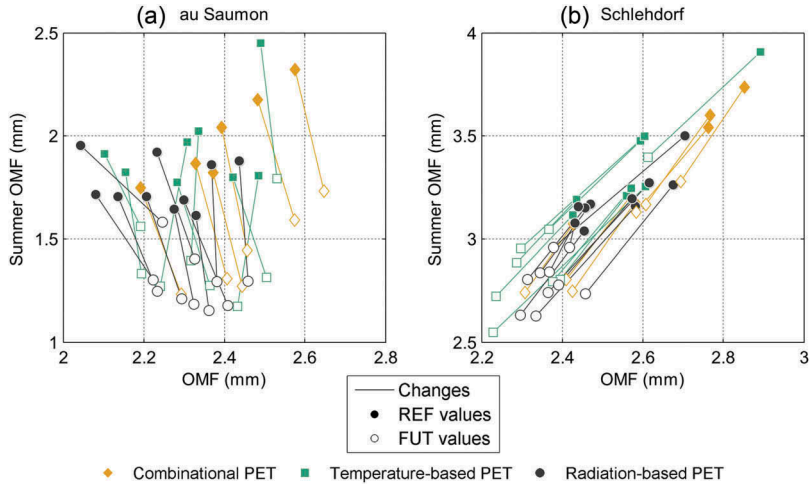

Figure 11. Overall mean flow (in mm, *x* axis) and summer overall mean flow (in mm, *y* axis) changes, from REF to FUT, for (a) au Saumon and (b) Schlehdorf.

combinational E_{02} (Penman-Monteith), while the lowest one is E_{21} (Abtew) for REF and E_{12} (MOHYSE) for FUT.

For Schlehdorf, the total discharge spread is 0.47 mm for REF and 0.47 mm for FUT. OMF decreases on average from 2.59 mm for REF to 2.40 mm for FUT. Combinational formulas show a total spread of 0.43 mm for REF and 0.39 mm for FUT, whereas spread is 0.47 mm and 0.38 mm, respectively, for temperature-based formulas. Again, radiation-based PET led to the lowest spread: 0.27 mm for REF and 0.16 mm for FUT. In fact, temperature-based E_{10} (Romanenko) is distinct, producing the highest OMF for REF and the second highest for FUT, after combinational E_{02} (Penman-Monteith).

Figure 10(b) illustrates summer OMF computed only for June, July and August. For au Saumon, the results reveal a change towards drier conditions for FUT: from 1.88 mm on average for REF to 1.36 mm for FUT. Summer OMF spread for REF ranges from 0.34 mm for radiation-based formulas to 0.68 mm for temperature-based ones, and 0.58 mm for combinational ones. FUT spread reaches 0.43 mm for radiation-based formulas, 0.62 mm for temperature-based ones, and 0.50 mm for combinational ones. The highest summer OMF, for both REF and FUT, are generated by temperature-based E_{10} (Romanenko), while the lowest is produced by radiation-based E_{17} (Jensen-Haise). For Schlehdorf, the summer OMF change is also towards drier conditions with on average 2.59 mm for REF and 2.40 mm for FUT. The REF spread is 0.66 mm for combinational formulas, 0.79 mm for temperature-based ones, and 0.46 mm for radiation-based ones. For FUT, these values reach 0.54 mm, 0.85 mm, and 0.33 mm, respectively. Again, E_{10} (Romanenko) is largely responsible for the high seasonal OMF temperature-based sensitivity. Lowest values are radiation-based E_{17} (Jensen-Haise) and temperature-based E_{14} (Kharrufa), respectively, for REF and FUT.

Resulting OMF changes for au Saumon are spread from +10% for radiation-based E_{21} (Abtew) to −2.9% for temperature-based E_{13} (Hydro-Québec). Similar statements can be made for Schlehdorf, with changes from −0.9% for E_{21} (Abtew) to −14.5% for E_{14} (Kharrufa). The summer OMF also shows large ranges for both catchments: from −18.35% (E_{08}) to −35.47% (E_{13}) for au Saumon and from −6.25% (E_{21}) to −21.66% (E_{14}) for Schlehdorf.

Figure 11 illustrates differences in terms of changes (solid lines) from REF (full symbols) to FUT (empty symbols) when plotting OMF and summer OMF. The picture of the impact of climate change on OMF and on summer OMF is blurred by the selection of a PET formula because they do not lead to the same evolution from REF to FUT. Indeed, identical changes would have resulted in solid lines parallel to one another, which is not strictly the case. Consequently, one cannot assert that arbitrarily selecting a PET formula would lead to a dependable OMF and seasonal OMF climate change impact assessment, even in the context for which one would only consider the change from REF to FUT and disregard the actual REF and FUT values. These results exemplify the influences of selecting a PET formula on the REF simulations and FUT projections as well as on the projected changes. They do not lead to the same results, which justifies the need for an evaluation of PET estimation options for projects assessing impacts of climate change on water resources.

4 Discussion and conclusions

Twenty-four potential evapotranspiration formulas were assessed under observed and projected climate conditions for natural catchments in Canada and Germany. The assessment employed a modelling chain composed of observed meteorological data, dynamically downscaled climatic projections, and a 20-member (ensemble) hydrological model fed with the PET formulas, along with a snow module. Appraisal aims to identify the origin of the sensitivity linked to PET formulas, discerning the propagation of the uncertainties up to the hydrological projections, and evaluating influences on the climate change impact conclusions for water resources based on daily averaged graphs, statistics and distribution tools, as well as hydrological indicators.

The 24 PET formulas produced large dissimilarities in the estimated PET in terms of quantity and shape. On one side, combinational formulas proposed very similar shapes and quantities; on the other side, temperature-based formulas

produced the largest spectrum of quantity. Radiation-based formulas fell somewhere in between the other two classes. These differences affected the resulting simulated discharge time series in several ways. Interestingly, when exploring the entire dataset for the calibration model—parameters that were used for projections—the highest model performance in terms of NSE_{sqrt} was achieved using locally developed formulas: the radiation-based E_{24} (Baier-Robertson) for Canada and the radiation-based E_{16} (Turc) for Western Europe. That same exercise confirmed that the multimodel led to less variability than the individual hydrological models, which was the largest for worse performing PET formulas. Overall, it was difficult to identify an ultimate PET formula from a hydrological modelling point of view, but avoiding temperature-based E_{08} and E_{12} could be recommended for the two studied watersheds.

The choice of the PET formula moderately affected the calibration efficiency, except for some formulas leading to much larger PET quantities than others, but hydrological models, during their calibration process, adapted their parameters so that efficiency was maximized. However, such adaptation influenced the entire simulated streamflow time series and not only the periods of higher PET quantities.

The analysis showed that selecting a PET formula has a strong influence on the conclusions that may be drawn from a hydrological climate change impact study. It might, however, be acknowledged that the present research only considers one future climate scenario. The sensitivity of the hydrological modelling to the PET formula turned out to be important for both catchments (as illustrated by the hydrological indicators, for example), in terms of simulated values and projected magnitudes of changes. PET formulas influenced FUT discharge over important dynamic periods such as spring high flows (snowmelt) for au Saumon, autumn high flows for Schlehdorf, and summer low flows in both locations. Events that were particularly impacted in future conditions include an anticipated spring flood (about 15 days earlier) with a lower peak, higher winter flows, and increased summer dryness, resulting in a reversal in the lower quantiles, especially for au Saumon.

Results also showed that spread of the hydrological response was smaller for the combinational formulas than for temperature-based and radiation-based equations, revealing a higher stability for these combinational formulas. Reasons for this stability were difficult to evaluate, but the closeness of the formulas and the use of various inner concepts affecting evaporative demand seem a probable explanation. This was already raised by Sheffield *et al.* (2012) and Trenberth et al. (2014) who mentioned that a more physically realistic calculation of evapotranspiration, which takes into account changes in available energy, humidity and wind speed, may result in smaller changes in water resources, especially when compared to temperature-based formulas. Further investigations of differing PET philosophies would be helpful to assess these results, as for example the "temperature-radiation assumption" (i.e. implicitly assuming a relationship between net radiation and temperature) mentioned in Hobbins *et al.* (2012) or the role of wind speed illustrated by Roderick *et al.* (2007).

The analysis of two hydrologically dissimilar catchments confirms past statements on the capacity of the calibration process to compensate differences in PET series. It also reveals that simulated streamflows are affected over the entire year due to this compensation in parameter identification. The projected impacts are thus influenced by the selection of a PET formula, with differences depending on the one selected.

It remains, however, to be demonstrated that this behaviour would be replicated on other catchments where the same methodology can be applied, perhaps with only an adaptation of selected PET formulas depending on local climate and available data. Also, the use of calibrated empirical PET parameters is questionable for future climatic conditions since the stability assumption of these coefficients can be a strong limitation. Further work on more contrasting watersheds on the hydro-climatic spectrum (e.g. water-limited catchments) would add interesting information on a wider range of climatic conditions and water management contexts.

This work, focusing on hydrological modelling, does not aim to provide water managers with the best PET formula for a specific watershed, because measured PET is not available in these catchments and also because a better PET series does not necessarily lead to a better discharge simulation. Instead, the assessment resorts to diverse available options for evapotranspiration estimation and comments on the impact of this choice on diagnosis of changes.

For a complete assessment of evaporative demand changes, further studies could include more complex impacts of climate change on transpiration controls (i.e. plant physiology, land-use change) besides meteorological controls. Their potential influence on impacts assessment has been illustrated by several researchers (e.g. Kay *et al.* 2013). This was not the case in this work due to the hydrological and lumped point of view of the study.

All the results reveal the importance of testing a large array of PET formulas as well as the need for neutral but efficient hydrological models. Moreover, the uncertainty analysis to PET selection confirms the need to identify how the sensitivity is propagated along the modelling process from simulated PET time series to decision-making indicators.

Acknowledgements

The authors thank partners in the QBIC[3] project, as well as the reviewers and editors for their valuable comments, discussions and references.

Disclosure statement

No potential conflict of interest was reported by the authors.

Funding

The authors acknowledge NSERC, Ouranos and Hydro-Québec for their support (grant RDCPJ 391616–09).

References

Abtew, W., 1996. Evapotranspiration measurements and modeling for three wetland systems in south Florida. *Journal of the American Water Resources Association*, 32 (3), 465–473. doi:10.1111/jawr.1996.32.issue-3

Allen, R.G., *et al.*, 1998. *Crop evapotranspiration - guidelines for computing crop water requirements - FAO irrigation and drainage paper 56*. Rome: FAO.

Allen, R.G., *et al*., 2005. *The ASCE standardized reference Evapotranspiration equation*. ASCE-EWRI Task Commitee Report. Reston, VA.

Andréassian, V., Perrin, C., and Michel, C., 2004. Impact of imperfect potential evapotranspiration knowledge on the efficiency and parameters of watershed models. *Journal of Hydrology*, 286, 19–35. doi:10.1016/j.jhydrol.2003.09.030

Bae, D.-H., Jung, I.-W., and Lettenmaier, D.P., 2011. Hydrologic uncertainties in climate change from IPCC AR4 GCM simulations of the Chungju Basin, Korea. *Journal of Hydrology*, 401, 90–105. doi:10.1016/j.jhydrol.2011.02.012

Baier, W. and Robertson, G.W., 1965. Estimation of latent evaporation from simple weather observations. *Canada Journal Soil Sciences*, 45, 276–284.

Baumgartner, A., Reichel, E., and Lee, R., 1975. *The world water balance: mean annual global, continental and maritime precipitation, evaporation and run-off*. Amsterdam: Elsevier.

Bell, V.A., *et al*., 2011. Estimating potential evaporation from vegetated surfaces for water management impact assessments using climate model output. *Journal of Hydrometeorology*, 12, 1127–1136. doi:10.1175/2011JHM1379.1

Bell, V.A., *et al*., 2012. How might climate change affect river flows across the Thames Basin? An area-wide analysis using the UKCP09 regional climate model ensemble. *Journal of Hydrology*, 442-443, 89–104. doi:10.1016/j.jhydrol.2012.04.001

Bergström, S. and Forsman, A., 1973. Development of a conceptual deterministic rainfall-runoff model. *Nordic Hydrology*, 4, 147–170.

Betts, R.A., *et al*., 2007. Projected increase in continental runoff due to plant responses to increasing carbon dioxide. *Nature*, 448, 1037–1041. doi:10.1038/nature06045

Beven, K.J. and Kirkby, M.J., 1979. A physically based, variable contributing area model of basin hydrology / Un modèle à base physique de zone d'appel variable de l'hydrologie du bassin versant. *Hydrological Sciences Bulletin*, 24 (1), 43–69. doi:10.1080/02626667909491834

Blaney, H.F. and Criddle, W.D., 1950. *Determining water requirements in irrigated areas from climatological and irrigation data*. Washington, DC: US Department of Agriculture, Soil Conservation Service, 48.

Boé, J., *et al*., 2009. Projected changes in components of the hydrological cycle in French river basins during the 21st century. *Water Resources Research*, 45, 1–15. doi:10.1029/2008WR007437

Bormann, H., 2011. Sensitivity analysis of 18 different potential evapotranspiration models to observed climatic change at German climate stations. *Climatic Change*, 104, 729–753. doi:10.1007/s10584-010-9869-7

Bos, M.G., *et al*., 2009. *Water requirements for irrigation and the environment*. Netherlands, Dordrecht: Springer.

Boyer, C., *et al*., 2010. Impact of climate change on the hydrology of St. Lawrence tributaries. *Journal of Hydrology*, 384, 65–83. doi:10.1016/j.jhydrol.2010.01.011

Brutsaert, W., 1982. *Evaporation into the atmosphere: theory, history and applications*. Dordrecht: Springer.

Burnash, R.J.C., 1995. The NWS river forecast system - catchment modeling. *In*: V.P. Singh, ed. *Computer models of watershed hydrology*. Highlands Ranch, CO: Water Resources Publications, 311–366.

Burnash, R.J.C., Ferral, R.L., and McGuire, R.A., 1973. *A generalized streamflow simulation system - conceptual modelling for digital computers*. Technical Report. Sacramento, CA: Joint Federal and State River Forecast Center.

Chen, J., *et al*., 2013. Finding appropriate bias correction methods in downscaling precipitation for hydrologic impact studies over North America. *Water Resources Research*, 49, 4187–4205. doi:10.1002/wrcr.20331

Chiew, F.H.S. and McMahon, T.A., 1994. Application of the daily rainfall-runoff model MODHYDROLOG to 28 Australian catchments. *Journal of Hydrology*, 153, 383–416. doi:10.1016/0022-1694(94)90200-3

Chiew, F.H.S., Peel, M.C., and Western, A.W., 2002. Application and testing of the simple rainfall–runoff model SIMHYD. *In*: V.P. Singh and D.K. Frevert, eds. *Mathematical models of small watershed hydrology and applications*. Littleton, Colorado: Water Resources Publication, 335–367.

Cormary, Y. and Guilbot, A., 1973. Étude des relations pluie-débit sur trois bassins versants d'investigation. *In*: *IAHS madrid symposium*. Vol. 108. IAHS Publication, 265–279. Paris: UNESCO.

De Elía, R. and Côté, H., 2010. Climate and climate change sensitivity to model configuration in the Canadian RCM over North America. *Meteorologische Zeitschrift*, 19, 325–339. doi:10.1127/0941-2948/2010/0469

Dibike, Y. and Coulibaly, P., 2005. Hydrologic impact of climate change in the Saguenay watershed: comparison of downscaling methods and hydrologic models. *Journal of Hydrology*, 307, 145–163. doi:10.1016/j.jhydrol.2004.10.012

Donohue, R.J., McVicar, T.R., and Roderick, M.L., 2010. Assessing the ability of potential evaporation formulations to capture the dynamics in evaporative demand within a changing climate. *Journal of Hydrology*, 386, 186–197. doi:10.1016/j.jhydrol.2010.03.020

Doorenbos, J. and Pruitt, W.O., 1977. Crop water requirements. *Irrigation and Drainage Paper No. 24*. Rome, Italy: FAO.

Duan, Q., Sorooshian, S., and Gupta, V., 1992. Effective and efficient global optimization for conceptual rainfall-runoff models. *Water Resources Research*, 28, 1015–1031. doi:10.1029/91WR02985

Duan, Q., Sorooshian, S., and Gupta, V., 1994. Optimal use of the SCE-UA global optimization method for calibrating watershed models. *Journal of Hydrology*, 158, 265–284. doi:10.1016/0022-1694(94)90057-4

Durre, I., *et al*., 2009. Radiosonde-based trends in precipitable water over the Northern Hemisphere: an update. *Journal of Geophysical Research*, 114, 1–8. doi:10.1029/2008JD010989

Edijatno, L. 1991. Mise au point d'un modèle élémentaire pluie-débit au pas de temps journalier. Thèse. Université Louis Pasteur de Strasbourg.

Ehret, U., *et al*., 2012. *HESS Opinions* "Should we apply bias correction to global and regional climate model data?". *Hydrology and Earth System Sciences*, 16 (9), 3391–3404. doi:10.5194/hess-16-3391-2012

Fischer, E.M. and Knutti, R., 2013. Robust projections of combined humidity and temperature extremes. *Nature Climate Change*, 3, 126–130. doi:10.1038/nclimate1682

Fisher, J.B., *et al*., 2005. Evapotranspiration models compared on a Sierra Nevada forest ecosystem. *Environmental Modelling & Software*, 20, 783–796. doi:10.1016/j.envsoft.2004.04.009

Fortin, V. and Turcotte, R., 2006. Le modèle hydrologique MOHYSE. *In*: *Note de cours pour SCA7420*. Département des sciences de la terre et de l'atmosphère, Montréal: Université du Québec à Montréal.

Fowler, A., 2002. Assessment of the validity of using mean potential evaporation in computations of the long-term soil water balance. *Journal of Hydrology*, 256, 248–263. doi:10.1016/S0022-1694(01)00542-X

Garçon, R., 1999. Modèle global Pluie-Débit pour la prévision et la prédétermination des crues. *La Houille Blanche*, 7, 88–95. doi:10.1051/lhb/1999088

Gardner, L.R., 2009. Assessing the effect of climate change on mean annual runoff. *Journal of Hydrology*, 379, 351–359. doi:10.1016/j.jhydrol.2009.10.021

Georgakakos, K.P., *et al*., 2004. Towards the characterization of streamflow simulation uncertainty through multimodel ensembles. *Journal of Hydrology*, 298, 222–241. doi:10.1016/j.jhydrol.2004.03.037

GIEC, 2007. *Bilan 2007 des changements climatiques. Contribution des Groupes de travail I, II et III au quatrième Rapport d'évaluation du Groupe d'experts intergouvernemental sur l'évolution du climat (Équipe de rédaction principale, Pachauri, R.K. et Reisinger, A.)*. GIEC: Genève, Suisse.

Girard, G., Morin, G., and Charbonneau, R., 1972. Modèle précipitations-débits à discrétisation spatiale, Cahiers ORSTOM. *Série Hydrologie*, IX (4), 35–52.

Hamon, W.R., 1961. Estimating potential evaporation. *In*: J.O.H. Division, ed. *Proceedings of the American society of civil engineers*. 107–120. Reston, VA: ASCE.

Hannachi, A., 2006. Quantifying changes and their uncertainties in probability distribution of climate variables using robust statistics. *Climate Dynamics*, 27, 301–317. doi:10.1007/s00382-006-0132-x

Hargreaves, G.H. and Samani, Z.A., 1985. Reference crop evapotranspiration from temperature. *Applied Engineering in Agriculture*, 1 (2), 96–99. doi:10.13031/2013.26773

Hobbins, M., *et al*., 2012. What drives the variability of evaporative demand across the conterminous United States? *Journal of Hydrometeorology*, 13, 1195–1214. doi:10.1175/JHM-D-11-0101.1

Hulme, M., Carter, T.R., and Viner, D., 1999. *Representing uncertainty in climate change scenarios and impact studies: ECLAT-2 workshop report no. 1*. Norwich: Climatic Research Unit.

Jakeman, A.J., Littlewood, I.G., and Whitehead, P.G., 1990. Computation of the instantaneous unit hydrograph and identifiable component flows with application to two small upland catchments. *Journal of Hydrology*, 117, 275–300. doi:10.1016/0022-1694(90)90097-H

Jensen, M. and Haise, H.R., 1963. Estimating evapotranspiration from solar radiation. *Journal of the Irrigation and Drainage Division - Proceedings of the American Society of Civil Engineers*, 89, 16–41.

Jensen, M.E., Burman, R.D., and Allen, R.G., 1990. *Evapotranspiration and irrigation water requirements*. Reston, VA: American Society of Civil Engineers.

Jones, R.N., *et al*., 2006. Estimating the sensitivity of mean annual runoff to climate change using selected hydrological models. *Advances in Water Resources*, 29, 1419–1429. doi:10.1016/j.advwatres.2005.11.001

Kannan, N., *et al*., 2007. Sensitivity analysis and identification of the best evapotranspiration and runoff options for hydrological modelling in SWAT-2000. *Journal of Hydrology*, 332, 456–466. doi:10.1016/j.jhydrol.2006.08.001

Kay, A.L., *et al*., 2013. A hydrological perspective on evaporation: historical trends and future projections in Britain. *Journal of Water and Climate Change*, 4 (3), 193–208. doi:10.2166/wcc.2013.014

Kay, A.L. and Davies, H.N., 2008. Calculating potential evaporation from climate model data: A source of uncertainty for hydrological climate change impacts. *Journal of Hydrology*, 358, 221–239. doi:10.1016/j.jhydrol.2008.06.005

Kay, A.L., *et al*., 2009. Comparison of uncertainty sources for climate change impacts: flood frequency in England. *Climatic Change*, 92 (1–2), 41–63. doi:10.1007/s10584-008-9471-4

Kharrufa, N.S., 1985. Simplified equation for evapotranspiration in arid regions. *Beiträge Zur Hydrologie Sonderheft*, 5 (1), 39–47.

Kingston, D.G., *et al*., 2009. Uncertainty in the estimation of potential evapotranspiration under climate change. *Geophysical Research Letters*, 36, L20403. doi:10.1029/2009GL040267

Kirchner, J.W., 2006. Getting the right answers for the right reasons: linking measurements, analyses, and models to advance the science of hydrology. *Water Resources Research*, 42, 1–5. doi:10.1029/2005WR004362

Lhomme, J.-P., 1997. Towards a rational definition of potential evaporation. *Hydrology and Earth System Sciences*, 1, 257–264. doi:10.5194/hess-1-257-1997

Linacre, E.T., 1977. A simple formula for estimating evaporation rates in various climates, using temperature data alone. *Agricultural Meteorology*, 18, 409–424. doi:10.1016/0002-1571(77)90007-3

Ludwig, R., *et al*., 2009. The role of hydrological model complexity and uncertainty in climate change impact assessment. *Advances In Geosciences*, 21, 63–71. doi:10.5194/adgeo-21-63-2009

Makkink, G.F., 1957. Testing the Penman formula by means of lysimeters. *Journal Institution Water Engineerings*, 11, 277–288.

Marke, T., 2008. *Development and application of a model interface to couple land surface models with regional climate models for climate change risk assessment in the upper danube watershed*. Munich: Ludwig-Maximilians-Universität München.

Mathevet, T., 2005. Quels modèles pluie-débit globaux au pas de temps horaire ? Thèse. École Nationale du Génie Rural, des Eaux et des Forêts.

Maurer, E.P., 2007. Uncertainty in hydrologic impacts of climate change in the Sierra Nevada, California, under two emissions scenarios. *Climatic Change*, 82, 309–325. doi:10.1007/s10584-006-9180-9

Mazenc, B., Sanchez, M., and Thiery, D., 1984. Analyse de l'influence de la physiographie d'un bassin versant sur les paramètres d'un modèle hydrologique global et sur les débits caractéristiques à l'exutoire. *Journal of Hydrology*, 69, 97–118. doi:10.1016/0022-1694(84)90158-6

McGuinness, J.L. and Bordne, E.F., 1972. *A comparison of lysimeter-derived potential evapotranspiration with computed values*. Technical Bulletin 1452. Washington, DC: Agricultural Research Service, US Department of Agriculture.

McKenney, M.S. and Rosenberg, N.J., 1993. Sensitivity of some potential evapotranspiration estimation methods to climate change. *Agricultural and Forest Meteorology*, 64, 81–110. doi:10.1016/0168-1923(93)90095-Y

McVicar, T.R., *et al*., 2012. Global review and synthesis of trends in observed terrestrial near-surface wind speeds: implications for evaporation. *Journal of Hydrology*, 416-417, 182–205. doi:10.1016/j.jhydrol.2011.10.024

McVicar, T.R., *et al*., 2008. Wind speed climatology and trends for Australia, 1975–2006: Capturing the stilling phenomenon and comparison with near-surface reanalysis output. *Geophysical Research Letters*, 35, 1–6. doi:10.1029/2008GL035627

Milly, P.C.D. and Dunne, K.A., 2011. On the hydrologic adjustment of climate-model projections: the potential pitfall of potential evapotranspiration. *Earth Interactions*, 15, 1–14. doi:10.1175/2010EI363.1

Minville, M., Brissette, F., and Leconte, R., 2008. Uncertainty of the impact of climate change on the hydrology of a nordic watershed. *Journal of Hydrology*, 358, 70–83. doi:10.1016/j.jhydrol.2008.05.033

Monteith, J.L., 1965. Evaporation and the environment. *In*: *The state and movement of water in living organisms, XIXth symposium*. Swansea: Cambridge University Press, 205–234.

Moore, R.J. and Clarke, R.T., 1981. A distribution function approach to rainfall-runoff modeling, water resources. *Research*, 17 (5), 1367–1382.

Morton, F.I., 1994. Evaporation research - a critical review and its lessons for the environmental sciences. *Critical Reviews in Environmental Science and Technology*, 24, 237–280. doi:10.1080/10643389409388467

Muerth, M.J., *et al*., 2013. On the need for bias correction in regional climate scenarios to assess climate change impacts on river runoff. *Hydrology and Earth System Sciences*, 17, 1189–1204. doi:10.5194/hess-17-1189-2013

Nakicenovic, N., *et al*., 2000. Emissions scenarios. *A Special Report of Working Group III of the Intergovernmental Panel on Climate Change*., Cambridge, UK: Cambridge University Press.

Nielsen, S.A. and Hansen, E., 1973. Numerical simulation of the rainfall-runoff process on a daily basis. *Nordic Hydrology*, 4, 171–190.

O'Connell, P.E., Nash, J.E., and Farrell, J.P., 1970. River flow forecasting through conceptual models, part II - The Brosna catchment at Ferbane. *Journal of Hydrology*, 10, 317–329. doi:10.1016/0022-1694(70)90221-0

Oudin, L., *et al*., 2006. Dynamic averaging of rainfall-runoff model simulations from complementary model parameterizations. *Water Resources Research*, 42, 10. doi:10.1029/2005WR004636

Oudin, L., *et al*., 2005b. Which potential evapotranspiration input for a lumped rainfall-runoff model? Part 2-Towards a simple and efficient potential evapotranspiration model for rainfall-runoff modelling. *Journal of Hydrology*, 303, 290–306. doi:10.1016/j.jhydrol.2004.08.026

Oudin, L., Michel, C., and Anctil, F., 2005a. Which potential evapotranspiration input for a lumped rainfall-runoff model? Part 1-can rainfall-runoff models effectively handle detailed potential evapotranspiration inputs? *Journal of Hydrology*, 303, 275–289. doi:10.1016/j.jhydrol.2004.08.025

Parmele, L.H., 1972. Errors in output of hydrologic models due to errors in input potential evapotranspiration. *Water Resources Research*, 8, 348–359. doi:10.1029/WR008i002p00348

Paturel, J.E., Servat, E., and Vassiliadis, A., 1995. Sensitivity of conceptual rainfall-runoff algorithms to errors in input data - case of the GR2M model. *Journal of Hydrology*, 168, 111–125. doi:10.1016/0022-1694(94)02654-T

Penman, H.L., 1948. Natural evaporation from open water, bare soil and grass. *In*: *Proceedings of the royal society of London. Series A. Mathematical and physical sciences 193*. London: The Royal Society. 120–145.

Perrin, C., Michel, C., and Andréassian, V., 2001. Does a large number of parameters enhance model performance? Comparative assessment

of common catchment model structures on 429 catchments. *Journal of Hydrology*, 242, 275–301. doi:10.1016/S0022-1694(00)00393-0

Perrin, C., Michel, C., and Andréassian, V., 2003. Improvement of a parsimonious model for streamflow simulation. *Journal of Hydrology*, 279 (1–4), 275–289. doi:10.1016/S0022-1694(03)00225-7

Priestley, C.H.B. and Taylor, R.J., 1972. On the assessment of surface heat flux and evaporation using large-scale parameters. *Monthly Weather Review*, 100, 81–92. doi:10.1175/1520-0493(1972)100<0081:OTAOSH>2.3.CO;2

Prudhomme, C., Jakob, D., and Svensson, C., 2003. Uncertainty and climate change impact on the flood regime of small UK catchments. *Journal of Hydrology*, 277, 1–23. doi:10.1016/S0022-1694(03)00065-9

Prudhomme, C. and Williamson, J., 2013. Derivation of RCM-driven potential evapotranspiration for hydrological climate change impact analysis in Great Britain: a comparison of methods and associated uncertainty in future projections. *Hydrology and Earth System Sciences*, 17, 1365–1377. doi:10.5194/hess-17-1365-2013

Roderick, M.L., *et al.*, 2007. On the attribution of changing pan evaporation. *Geophysical Research Letters*, 34, L17403. doi:10.1029/2007GL031166

Romanenko, V.A., 1961. Computation of the autumn soil moisture using a universal relationship for a large area. *In*: *Proceedings Ukrainian Hydrometeorological Research Institute (Kiev)*. Kiev: Ukrainian Hydrometeorological Research Institute, 3.

Schmidli, J., Frei, C., and Vidale, P.L., 2006. Downscaling from GCM precipitation: a benchmark for dynamical and statistical downscaling methods. *International Journal of Climatology*, 26, 679–689. doi:10.1002/(ISSN)1097-0088

Seiller, G. and Anctil, F., 2014. Climate change impacts on the hydrologic regime of a Canadian river: comparing uncertainties arising from climate natural variability and lumped hydrological model structures. *Hydrology and Earth System Sciences*, 18, 2033–2047. doi:10.5194/hess-18-2033-2014

Seiller, G., Anctil, F., and Perrin, C., 2012. Multimodel evaluation of twenty lumped hydrological models under contrasted climate conditions. *Hydrology and Earth System Sciences*, 16, 1171–1189. doi:10.5194/hess-16-1171-2012

Seiller, G., Hajji, I., and Anctil, F., 2015. Improving the temporal transposability of lumped hydrological models on twenty diversified U.S. watersheds. *Journal of Hydrology: Regional Studies*, 3, 379–399.

Sheffield, J., Wood, E.F., and Roderick, M.L., 2012. Little change in global drought over the past 60 years. *Nature*, 491, 435–438. doi:10.1038/nature11575

Singh, V.P., 1989. *Hydrologic systems: watershed modeling - volume 2*. Englewood Cliffs, NJ: Prentice Hall.

Singh, V.P. and Xu, C.-Y., 1997a. Evaluation and generalization of 13 mass transfer equations for determining free water evaporation. *Hydrological Processes*, 11, 311–323. doi:10.1002/(ISSN)1099-1085

Singh, V.P. and Xu, C.-Y., 1997b. Sensitivity of mass transfer-based evaporation equations to errors in daily and monthly input data. *Hydrol Processing*, 11, 1465–1473. doi:10.1002/(ISSN)1099-1085

Sperna Weiland, F.C., *et al.*, 2012. Selecting the optimal method to calculate daily global reference potential evaporation from CFSR reanalysis data for application in a hydrological model study. *Hydrology and Earth System Sciences*, 16, 983–1000. doi:10.5194/hess-16-983-2012

Sugawara, M., 1979. Automatic calibration of the tank model / L'étalonnage automatique d'un modèle à cisterne. *Hydrological Sciences Bulletin*, 24 (3), 375–388. doi:10.1080/02626667909491876

Thiery, D., 1982. *Utilisation d'un modèle global pour identifier sur un niveau piézométrique des influences multiples dues à diverses activités humaines*, Vol. 136. Exeter: IAHS Publication, 71–77.

Thom, A.S. and Oliver, H.R., 1977. On Penman's equation for estimating regional evaporation. *Quarterly Journal of the Royal Meteorological Society*, 103, 345–357. doi:10.1002/(ISSN)1477-870X

Thornthwaite, C.W., 1948. An approach toward a rational classification of climate. *Geographical Review*, 38, 55. doi:10.2307/210739

Thornthwaite, C.W. and Mather, J.R., 1955. *The water balance, publications in climatology*. Vol. 8(1). Centerton, NJ: Drexel Institute of Climatology, 1–104.

Trenberth, K.E., *et al.*, 2014. Global warming and changes in drought. *Nature Climate Change*, 4, 17–22. doi:10.1038/nclimate2067

Turc, L., 1955. Le bilan d'eau des sols. Relations entre les précipitations, l'évaporation et l'écoulement. *Annals Agriculture*, 6, 5–131.

Valéry, A., Andréassian, V., and Perrin, C., 2014. 'As simple as possible but not simpler': what is useful in a temperature-based snow-accounting routine? Part 2 - Sensitivity analysis of the Cemaneige snow accounting routine on 380 catchments. *Journal of Hydrology*, 517, 1176–1187. doi:10.1016/j.jhydrol.2014.04.058

Velázquez, J.A., Anctil, F., and Perrin, C., 2010. Performance and reliability of multimodel hydrological ensemble simulations based on seventeen lumped models and a thousand catchments. *Hydrology and Earth System Sciences*, 14, 2303–2317. doi:10.5194/hess-14-2303-2010

Velázquez, J.A., *et al.*, 2011. Can a multi-model approach improve hydrological ensemble forecasting? A study on 29 French catchments using 16 hydrological model structures. *Advances in Geosciences*, 29, 33–42. doi:10.5194/adgeo-29-33-2011

Verstraeten, W.W., Veroustraete, F., and Feyen, J., 2008. Assessment of evapotranspiration and soil moisture content across different scales of observation. *Sensors*, 8, 70–117. doi:10.3390/s8010070

Vicuna, S., *et al.*, 2007. The sensitivity of California water resources to climate change scenarios. *Journal of the American Water Resources Association*, 43, 482–498. doi:10.1111/jawr.2007.43.issue-2

Wagener, T., *et al.*, 2001. A framework for development and application of hydrological models. *Hydrology and Earth System Sciences*, 5 (1), 13–26. doi:10.5194/hess-5-13-2001

Warmerdam, P.M.M., Kole, J., and Chormanski, J., 1997. Modelling rainfall-runoff processes in the Hupselse Beek research basin, Ecohydrological processes in small basins. *In*: *Proceedings of the Strasbourg Conference (24-26 September 1996), IHP-V, Technical Documents in Hydrology*. Vol. 14. Paris: UNESCO, 155–160.

Wilcox, R.R., 1997. *Introduction to robust estimation and hypothesis testing*. 1st ed. New York: Academic Press.

Wild, M., 2009. Global dimming and brightening: A review. *Journal of Geophysical Research*, 114, 1–31. doi:10.1029/2008JD011470

Wilks, D.S., 2011. *Statistical methods in the atmosphere sciences*. 3rd ed. San Diego, CA: Academic press.

Wright, J.L., 1982. New evapotranspiration crop coefficients. *Journal of Irrigation and Drainage Engineering*, 108 (IR2), 57–74.

Xu, C.-Y. and Singh, V.P., 2000. Evaluation and generalization of radiation-based methods for calculating evaporation. *Hydrological Processes*, 14, 339–349. doi:10.1002/(ISSN)1099-1085

Xu, C.-Y. and Singh, V.P., 2001. Evaluation and generalization of temperature-based methods for calculating evaporation. *Hydrological Processes*, 15, 305–319. doi:10.1002/(ISSN)1099-1085

Xu, C.-Y. and Singh, V.P., 2002. Cross comparison of empirical equations for calculating potential evapotranspiration with data from Switzerland. *Water Resources Management*, 16, 197–219. doi:10.1023/A:1020282515975

Zhao, R.J., *et al.*, 1980. *The Xinanjiang model*, Vol. 129. Wallingford, UK: IAHS Publication, 351–356.

Appendix

Potential evapotranspiration formulas

E_{01} : Penman (1948)

$$\mathrm{PET} = \frac{\Delta R_n + \gamma(e_s - e_a).2.62(1 + 0.537U)}{\lambda(\Delta + \gamma)}$$

E_{02} : Penman-Monteith (Monteith, 1965)

$$\mathrm{PET} = \frac{\Delta R_n + \left[86400.d_a.C_p(e_s - e_a)\right].\frac{1}{r_a}}{\lambda\left[\Delta + \gamma\left(1 + \frac{r_s}{r_a}\right)\right]}$$

E_{03} : FAO56 P-M (Allen *et al.*, 2005)

$$\text{PET} = \frac{0.408.\Delta R_n + \gamma\left(\frac{900}{T_a+273}\right).U(e_s - e_a)}{\Delta + \gamma(1 + 0.34U)}$$

E_{04} : Priestley and Taylor (1972)

$$\text{PET} = \frac{\alpha_{pt}\Delta R_n}{\lambda\rho(\Delta + \gamma)}, \text{with } \alpha_{pt} = 1.26$$

E_{05} : Kimberly-Penman (Wright, 1982)

$$\text{PET} = \frac{\frac{\Delta}{\Delta+\gamma}R_n + 2.62\left(\frac{\gamma}{\Delta+\gamma}\right).(e_s - e_a).K}{\lambda}$$

$$\text{with } K = \left[0.4 + 0.14\exp\left(-\left(\frac{J_D - 173}{58}\right)^2\right)\right] + \left[0.605 + 0.345\exp\left(-\left(\frac{J_D - 243}{80}\right)^2\right)\right]U$$

E_{06} : Thom and Oliver (1977)

$$\text{PET} = \frac{\Delta R_n + 2.5\gamma(e_s - e_a).2.62(1 + 0.536U)}{\lambda\rho\left(\Delta + \gamma\left(1 + \frac{r_s}{r_a}\right)\right)}$$

E_{07} : Thornthwaite (1948)

$$\text{PET} = 16\left(\frac{\text{DL}}{360}\right)\left(\frac{10T_a}{I}\right)^K$$

$$\text{with } I = \sum_{n=1}^{12}\left(\frac{T_k}{5}\right)^{1.514} \text{ where } T_k \text{ is the mean monthly temperature}$$

$$\text{and } K = 0.49239 + 1.792.I.10^{-2} - 0.771.I^2.10^{-4}$$

E_{08} : Blaney and Criddle (1950)

$$\text{PET} = k\left(100.\frac{\text{DL}}{365 \times 12}\right).(0.46.T_a + 8.13)$$

with k varying from 0.45 to 1.2 according to season and vegetation

E_{09} : Hamon (1961)

$$\text{PET} = \left(\frac{\text{DL}}{12}\right)^2 \exp\left(\frac{T_a}{16}\right)$$

E_{10} : Romanenko (1961)

$$\text{PET} = 4.5\left(1 + \frac{T_a}{25}\right)^2\left(1 - \frac{e_a}{e_s}\right)$$

E_{11} : Linacre (1977)

$$\text{PET} = \frac{\frac{500(T_a+0.006z)}{100-Lat} + 15(T_a - T_d)}{80 - T_a}$$

with Lat the latitude of the station and z the altitude (m)

E_{12} : MOHYSE (Fortin and Turcotte, 2006)

$$\text{PET} = \frac{4.088}{\pi}.\omega.\exp\left(\frac{17.3T_a}{238 + T_a}\right)$$

with ω the sunset hour angle (rad)

E_{13} : Hydro-Québec – HSAMI

$$\text{PET} = 0.02978(T_{\max} - T_{\min})\exp\left(0.019\left(\frac{9}{5}(T_{\max} + T_{\min}) + 64\right)\right)$$

E_{14} : Kharrufa (1985)

$$\text{PET} = 0.34\left(100.\frac{\text{DL}}{365 \times 12}\right).T_a{}^{1.3}$$

E_{15} : Wendling – WASim (1975)

$$\text{PET} = 100R_s(1.1 - \alpha) + 93.f_k.\left(\frac{T_a + 22}{150(T + 123)}\right), \text{with } f_k = 0.8$$

E_{16} : Turc (1955)

$$\text{PET} = 1000.\frac{1}{\lambda\rho}.\left(\frac{T_a}{T_a + 15}\right).\frac{(R_s(1 - \alpha) + 24)}{1.3}.c$$

$$\text{with } c = 1 + \frac{50 - \text{RH}}{70} \text{ for RH}<50\%;\ c = 1 \text{ for RH} \geq 50\%$$

E_{17} : Jensen and Haise (1963)

$$\text{PET} = 1000.\frac{R_e}{\lambda\rho}.\frac{T_a}{40}$$

E_{18} : McGuinness and Bordne (1972)

$$\text{PET} = 1000.\frac{R_e}{\lambda\rho}.\frac{T_a + 5}{68}$$

E_{19} : Hargreaves and Samani (1985)

$$\text{PET} = 0.0023.\frac{R_e}{\lambda\rho}.\sqrt{(T_{\max} - T_{\min})}.(T_a + 17.8).1000$$

E_{20} : Doorenbos and Pruitt (1977)

$$\text{PET} = K.\frac{1}{\lambda}.\frac{\Delta R_s}{\Delta + \gamma} - 0.3$$

$$\text{with } K = 1.066 - 0.13\frac{\text{RH}}{100} + 0.045U - 0.02\frac{\text{RH}}{100}U - 0.00315\left(\frac{\text{RH}}{100}\right)^2 - 0.0011U^2$$

E_{21} : Abtew (1996)

$$\text{PET} = 0.53\frac{R_s}{\lambda\rho}(1 - \alpha).1000$$

E_{22} : Makkink (1957)

$$\text{PET} = \left(0.61.\frac{1}{\lambda}.\frac{\Delta}{\Delta + \gamma}.\frac{R_s}{58.5} - 0.012\right) \times 100$$

E_{23} : Oudin (2005)

$$\text{PET} = 1000.\frac{R_e}{\lambda\rho}.\frac{T_a + 5}{100}$$

E_{24} : Baier and Robertson (1965)

$$\text{PET} = 0.157T_{\max} + 0.158(T_{\max} - T_{\min}) + 0.109R_e - 5.39$$

Notation and units

PET	Potential evapotranspiration (mm d^{-1})
Δ	Slope of vapor pressure curve (kPa °C^{-1})
λ	Latent heat of vaporization (MJ kg^{-1})
ρ	Water density (=1000 kg L^{-1})
d_a	Air density (kg m^{-3})
γ	Psychrometric constant (kPa °C^{-1})
e_s	Saturation vapour pressure (kPa)
e_a	Actual vapour pressure (kPa)
r_a	Aerodynamic resistance (s m^{-1})
r_s	Surface resistance of reference crop (= 70 s m^{-1})
U	Wind speed 2 m above soil surface (m s^{-1})
T_a	Air temperature (°C)
T_d	Dew point temperature (°C)
$T_{\max}$	Maximum air temperature (°C)
$T_{\min}$	Minimum air temperature (°C)
R_e	Extraterrestrial radiation (MJ m^{-2} d^{-1})
R_s	Global short-wave radiation (MJ m^{-2} d^{-1})
R_n	Net incoming solar radiation (MJ m^{-2} d^{-1})
RH	Relative humidity (%)
DL	Day length (h d^{-1})
α	Surface albedo (-)
J_D	Julian day (ordinal date)
C_p	Air specific heat capacity (= $1.013.10^{-3}$ MJ kg^{-1} °C^{-1})